you don't need a weatherman to know which way the wind blows

a blog

(baroclinic instability, and what to do about it)

siminos/baroclinic/BrCv12.tex, rev. 3011: last edit by Predrag Cvitanović,

04/01/2013

Sebastian Ortega Arango, Annalisa Bracco and Predrag Cvitanović

May 5, 2022

Contents

Chapter 1

Baroclinic flows

To view just the project (without this line and the blog) toggle the `boyscoutfalse` switch, towards the top of `siminos/baroclinic/BrCv12.tex` file.

1.1 Introduction

[1] The concept of baroclinic instability is perhaps one of the harder ones to grasp in geophysical fluid mechanics. However, it is also one of the most fundamental concepts on this field, as it is the main driver for the large scale circulations in the atmosphere and important circulations in the ocean. It is by this mechanism that the atmosphere redistributes heat from low latitudes to high latitudes, that it sustains synoptic weather system and by which some oceanic eddies develop. Its importance can not be overstated.

[2] On the other hand, one could argue that the study of baroclinic flows remains in its early stages. Although there exist a very well developed linear theory for the onset of this type of instability, there still much room to explore the nonlinear regimes. A way to approach this studies is given by recent advances in the dynamical approaches to study of turbulence [1, 2, 3]; [3] making use of the symmetries of the system, and finding periodic orbits and fixed points, as a way to understand the manifold of this type of setups.

In this study we introduce the physics and present some of the nonlinear theory methods that might be used to analyze baroclinic flows. We will briefly mention insights from stability theory, but the emphasis would not be on them. Great papers and books have already been written about it.

The work is divided as follows. In sect. 1.2 we introduce the problem in a qualitative matter, hoping that this simple approach illuminates the underlying physical

[1] Sebastian: Not really sure if it is the hardest one to understand. But I remembered it seem to distant to me the first time the concept was introduced to me.

[2] Sebastian: Here I am mostly speculating. However, this is the impression I have so far

[3] Sebastian: pick appropriate references here. Predrag: cite ref. [4] when you introduce symmetry reduction

principles. In sect. 1.3 we use Navier-Stokes equation to derive the vorticity equation and explicitly expose the the baroclinic term which is the cause of this instability. In sect. 1.4 we introduce the QG-Equations, which are a simplified set of equations suitable to study of geophysical flows. Sect. 1.5 introduces some basic techniques for showing how the stability of such flows might be addressed. Finally, the remainder of this study is devoted to show how nonlinear techniques can be used to identify important properties of this types of flows.

1.2 Qualitative Examples

[4] The simple example which we develop here illustrates the mechanism initiating baroclinic flows. To start with, let us ignore the effects due to earths rotation and concentrate only in inertial frames. That is, let's start not by treating baroclinic instability perse, but the process by which a fluid adjust to equilibrium given a uneven distribution in density. A great example of this is Marsigli's experiment to explain undercurrent flows in the Bosphorus river from the Mediterranean to the Black Sea (see ref. [5]), and we will begin with a gedanken experiment based on this.

Consider the situation shown in figure 1.1.a, where two fluids of different densities, initially separated at x_0, are suddenly allowed to interact. The situation is clearly unstable; a pressure gradient would exist at all levels, except for the surface, going from the heavier fluid to the lighter one. This would create both subsurface and surface currents, one due to the pressure gradient in the bottom, and the other due to mass conservation in the surface. Intuitively we can imagine that the system would finally settle to a configuration where the heavier fluid would lay on the bottom and the lighter one on top. That is, a configuration where the potential energy is minimized.

Thinking about this problem in terms of surface of constant pressure and density we can understand the instability that causes this type of behavior. In the initial configuration, the isopycnals are orthogonal to the isobars (see figure 1.1.b), so that the mentioned pressure gradient is generated at x_0. Later, as the denser fluid starts to settle in the lower layer, this pressure gradient starts to spread out; but it will always exist as long as there is a inclination is the isopycnals. At the end, when all the transient motions are settled and equilibrium is reached, both the isobars and the isopycnals are parallel; leaving the system in a lower potential energy state. A fundamental concept can be extracted from this:

> *In the absence of rotation, and an external forcing, equilibrium of a fluid is reached when isopycnals and isobars are parallel to each other.*

If this condition is not met, transient motions would be generated to extract the excess potential energy, and leave the system in its lower energy state.

The term responsible for the instability is quantified mathematically as the curl between the density and pressure gradients, that is:

$$\nabla\rho \times \nabla p\,, \tag{1.1}$$

[4] Sebastian: Just a rough draft, would continue to work soon.

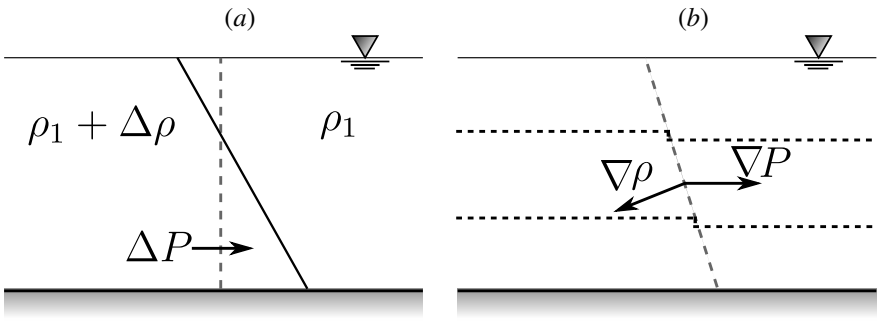

Figure 1.1: (a) Adjustment of a fluid subject to a horizontal difference in density in a non-rotating frame. (b) Isopycnals and isobars (dashed lines), and the pressure and density gradient for a unstable condition.

as we will show in sect. 1.3. Obviously, this definition agrees with the intuitively notion we just developed.

Consider now a further complication, and think about what would happen if the frame of reference were to be rotating in our previous experiment. In that case we would have to consider the apparent forces that develop on the individual fluid parcels of our flow, one proportional to the position (the centrifugal acceleration) and other proportional to the velocity (the Coriolis force) of each parcel. However, in geophysical applications the former one is often unimportant[5] [6], and only the effects of the Coriolis force need to be considered. Thus, if we repeat our experiment from a initial state as before, the motion of the fluid would be determined by the effects of the pressure gradient and the Coriolis force.

In this new setup, each individual parcel starts moving due to the pressure gradient force but the presence of rotation makes them deviate from a straight trajectory; as Coriolis force acts at right angles of the parcel velocity. Once these transient motions disappear, an new balanced state is reached, where the velocity becomes perpendicular to the pressure gradient force (see figure 1.2). This balance state is referred commonly as geostrophic balance, and it differs from the previous example in that in this new balance the pressure gradient does not vanishes, but rather is balanced by the Coriolis force. That is, from the inviscid, unforced Navier-Stokes equations one would get:

$$\mathbf{u}_g = -\frac{1}{f\rho}\mathbf{k} \times \nabla_z p\,, \tag{1.2}$$

where $\mathbf{u}_g$ is the horizontal component of the velocity, f is the Coriolis parameter, ρ is the density of the flow, p is the pressure and g the acceleration due to gravity. In addition, the use of the hydrostatic relation implies the following relation for the change

[5] Due to the departure from sphericity of the earth

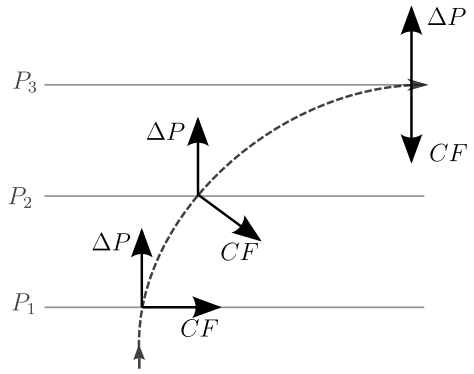

Figure 1.2: Process of geostrophic adjustment for an initially motionless fluid parcel.

in the vertical; which is commonly referred as the thermal wind equation [7]: [6]

$$\begin{aligned} \frac{\partial \rho u_g}{\partial p} &= \frac{1}{f}\left(\frac{\partial \alpha}{\partial y}\right) \\ \frac{\partial \rho u_g}{\partial p} &= -\frac{1}{f}\left(\frac{\partial \alpha}{\partial x}\right), \end{aligned} \tag{1.3}$$

where α is the specific volume of the fluid.

From these relations, one concludes that there is a equilibrium state, in the presence of rotation, where the isopycnals and isobars are not necessarily parallel to each other. Nonetheless, instability occurs when the isopycnal slope exceeds a critical value; this type of phenomena is referred as baroclinic instability (see ref. [7]).

But which are the stability properties of this equilibrium, and the motions that are generated afterwards? The first question has been studied widely, and it uses linear approximations to develop the relations between flow properties that need to be meet in order for it to remain stable, or become unstable. The study of the motions that develops after the initial instability is a more challenging problem as nonlinear terms now become important. The hope is that nonlinear theory allow us to extract important knowledge about this phenomena even in high dimensional simulations.

1.3 Vorticity Equation

What is clear from Marsigli's experiment, is that the impact of the solenoidal term is to induce vorticity in the fluid[7]. This variable is a fundamental property of the fluid, and studying it has the power of greatly simplify the analysis of a given flow. In fact, the

[6] Predrag: many of your equations are split into pieces - here is an example how to put the together, have a single citation to them, in this case (1.3)

[7] The reader is referred to ref. [8] for an introductory, yet rigorous treatment of vorticity. However, be aware that in Kundu's derivation of the vorticity equation the density is not treated as a function of both pressure and temperature, but only of pressure; so that the solenoidal term is not considered.

first satisfactory attempts to model the atmosphere where done by Charney considering the vorticity of quasigeostrophic flows.

Vorticity arises naturally from Navier-Stokes equations, and is just a measure of the rotational speed of the fluid parcel. To make the derivation explicitly, let's consider the inviscid equations of motion in a rotating frame of reference[8], that is:

$$\frac{\partial \mathbf{u}}{\partial t} + (\mathbf{u}\cdot\nabla)\mathbf{u} + 2\Omega \times \mathbf{u} = -\frac{1}{\rho}\nabla p\,. \tag{1.4}$$

From vector calculus we note that:

$$(\mathbf{u}\cdot\nabla)\mathbf{u} = \frac{\nabla(\mathbf{u}\cdot\mathbf{u})}{2} - \mathbf{u}\times\omega \tag{1.5}$$

where ω is the vorticity. So that we can rewrite Navier-Stokes equation in the following way:

$$\frac{\partial \mathbf{u}}{\partial t} + (\omega + 2\Omega) \times \mathbf{u} = -\frac{1}{\rho}\nabla p - \frac{\mathbf{u}\cdot\mathbf{u}}{2} \tag{1.6}$$

Taking the curl of this equation (noting that $\omega = \nabla \times \mathbf{u}$) gives:

$$\frac{\partial \omega}{\partial t} + \nabla \times ((\omega + 2\Omega) \times \mathbf{u}) = -\nabla \times \left(\frac{1}{\rho}\nabla p\right) - \nabla \times \frac{\mathbf{u}\cdot\mathbf{u}}{2} \tag{1.7}$$

Finally using the identity $\nabla\times(A\times B) = A(\nabla\cdot B) - B(\nabla\cdot A) + (B\cdot\nabla)A - (A\cdot\nabla)B$, the chain rule for the pressure $\frac{1}{\rho}\nabla p = \nabla(p/\rho) - p\nabla(1/\rho)$, and the fact that the curl of a gradient is zero, the desired expression for the vorticity it is obtained from (1.6) (see ref. [7]). That is:

$$\frac{d}{dt}\left(\frac{\omega_a}{\rho}\right) = \left[\left(\frac{\omega_a}{\rho}\right)\cdot\nabla\right]\mathbf{u} + \nabla p \times \nabla\left(\frac{1}{\rho}\right) \tag{1.8}$$

where $\omega_a = \omega + 2\Omega$ is the absolute vorticity. It is then evident from this equations how the baroclinic term ($\nabla p \times \nabla(1/\rho)$) can induce vorticity in the fluid by means of the instabilities previously discussed.

Equation (1.8) can also be written for a single layer shallow water system as (see ref. [9]):

$$\frac{d}{dt}\left(\frac{\eta + f}{h}\right) = 0\,, \tag{1.9}$$

where η is the vertical component of the vorticity, h the instantaneous depth of the fluid, and the quantity conserved is referred as potential vorticity ($q = (\eta + f)/h$). A generalization to two or more layers is straight forward (see refs. [9, 10]). Simplified form of this expression, filtering unimportant motions for the large scale circulations is developed next for a two layer system. However, the equations would be rich in dynamics as advection terms are retained for the horizontal (so that a lot of interesting nonlinearities remains). Up to the date there still much interesting features of this system to be studied. [9]

[8] As explained in Section 1.1, only the Coriolis' force ($\Omega \times \mathbf{u}$) is considered in the equations, as the centripetal acceleration due to earths rotation can be ignored.

[9] Sebastian: I could include here a discussion about Kelvin circulation theorem, and how the baroclinic term would induce currents such as the sea breeze. However, I think I am extending a little to much in the basics. Hopefully this would make the project more readable.

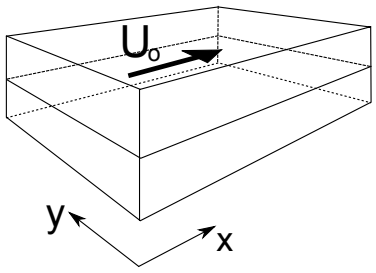

Figure 1.3: The geometry of the computational cell. Two layer quasigeostrophic model with vertical shear characterized by U_o, x the streamwise, and y the spanwise coordinate. The geophysically relevant case is a channel whose zonal (streamwise) length is substantially greater than its meridional (spanwise) breadth.

1.4 2 Layer QG-Equations

If we intend to study baroclinic instability, we need to be able to capture two basic properties of the flow (as shown in sect. 1.2): the nearly geostrophic motions of the fluid and its vertical structure as given by (1.3). One of the simplest mathematical systems that would capture this type of behavior ref. [10], is a quasigeostrophic set of equations discretized for two vertical layers. A quick derivation is given here[10]. For in-depth derivations the reader is referred to refs. [9, 6, 7, 10].

The geometry of the computational cell is sketched in figure 1.3. [11]

Consider the situation in figure 1.4, where we have two layers of different densities, equal depths H, and the Rossby number is small enough so that we can use the quasigeostrophic approximation. The potential vorticity of each layer can then be written as:

$$q_i = \frac{\eta_i + f}{h_i} \,, \tag{1.10}$$

where η_i is the relative vorticity of each layer, f the planetary vorticity and h_i distance

[10] We follow a intuitively approach for the sake of simplicity. However a much more systematic derivation can be made with asymptotic methods and the reader is advise to explore them (see for instance refs. [9, 11, 12]), as they expose how different approximations relate to each other.

[11] Predrag: 2012-06-13 Predrag: incorporate/merge this into your writeup: " In this work, the baroclinic instability is modeled by a 2-layer incompressible viscous fluid in a channel with no-slip side walls, periodic in streamwise direction, top layer driven by 'atmospheric stream', i.e. a constant total streamwise volume flow per unit time. We impose uniform streamwise velocity of unit size, ignoring the boundary condition (probably one should use a parabolic profile). With free slip the layers are still unstable in the same way, just the boundary behavior is different. Oceanographers prefer no-slip, perhaps because of coastal stream. The bottom layer is not forced, no slip, no Ekman layer (Ekman layer models friction at the bottom; that would make sense when one works with 50 layers, but not two). The two layers are coupled by the difference $\Phi_2 - \Phi_1$. Laplacian of stream function is vorticity. Each layer is computed in terms of vorticity equations as a 2-dimensional fluid. The lower layer has higher fluid density, and they are coupled across their interface by difference of vorticity.

In our simulation this is about factor two; it is related to the Rösby deformation radius L_R. The spanwise y width is $L_R/2\pi = 1/2$. Unless the width is larger than L_R, no instability. The stream-wise aspect ration is about 8. "

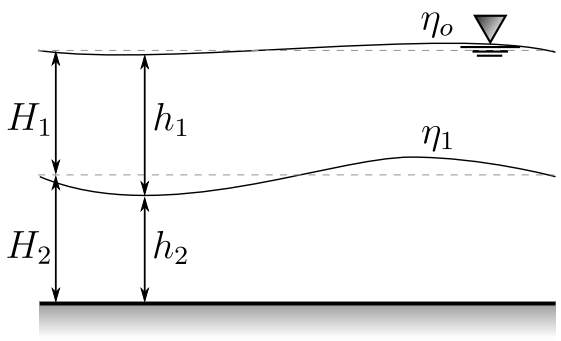

Figure 1.4: Two layer model considered in the simulations.

between layers[12]. As we learned, this property must be conserved by each layer, then:

$$\frac{dq_i}{dt} = \frac{d}{dt}\left(\frac{\eta_i + f}{h_i}\right) \simeq \frac{d}{dt}\left(f + \eta_i - f\frac{h_i'}{H_i}\right) = 0\,, \tag{1.11}$$

where the approximation is only valid when Rossby number is small. H_i is the unperturbed layer thickness, and h_i' is the thickness perturbation for layer i. Now let us introduce the geostrophic equations to approximate the wind and the vorticity.

First note that from (1.2) that the velocities only depend on the pressure gradient, and that the fluid can be regarded as incompressible if we assume that the vertical gradient of w is small. Then the pressure will depend only depend on the height of the interfaces. An it can in turn be related to h_i. That is, the height of the surfaces is given by:

$$\eta_o = h_1 + h_2 = h_1' + h_2' + 2H \tag{1.12}$$

$$\eta_1 = h_2 = h_2' + H \tag{1.13}$$

so that the pressure in the first layer is given by:

$$p = g\rho_1(\eta_o - z)\,, \tag{1.14}$$

and the horizontal gradient is:

$$\nabla p = g\rho_1\nabla\eta_o = g\rho_1(\nabla h_1' + \nabla h_2') \tag{1.15}$$

With the same procedure it is found for the second layer:

$$\nabla p = g\rho_1(\nabla h_1' + \nabla h_2') + g'\rho_1\nabla h_2'\,, \tag{1.16}$$

where $g' = (\rho_2 - \rho_1)/\rho_1$ is the reduced gravity. The geostrophic condition then gives for the top layer:

$$u_g = -\frac{g}{f}\frac{\partial}{\partial y}(h_1' + h_2') \tag{1.17}$$

[12] We follow the derivation and the notation of ref. [9]

$$v_g = \frac{g}{f}\frac{\partial}{\partial x}(h_1' + h_2')\,, \tag{1.18}$$

and for the bottom layer:

$$u_g = -\frac{g}{f}\frac{\partial}{\partial y}(h_1' + h_2') - \frac{g'}{f}\frac{\partial h_2'}{\partial y} \tag{1.19}$$

$$v_g = \frac{g}{f}\frac{\partial}{\partial x}(h_1' + h_2') + \frac{g'}{f}\frac{\partial h_2'}{\partial x} \tag{1.20}$$

From the equations above, it is clear that the equations can be written in terms of a stream function for each layer, such that $u_i = -\partial\psi_i/\partial y$, $v_i = \partial\psi_i/\partial x$ and the vorticity is simply written as $\eta_i = \nabla^2\psi_i$, with the stream functions

$$\psi_1 = \frac{g}{f}(h_1' + h_2') \tag{1.21}$$

$$\psi_2 = \frac{g}{f}(h_1' + h_2') + \frac{g'h_2'}{f}\,. \tag{1.22}$$

An expression for the potential vorticity of each layer in terms of the stream functions, is obtained if we use these in (1.11):

$$q_1 = \beta y + \nabla^2\psi_1 + \frac{f_o^2}{g'H}(\psi_2 - \psi_1) - \frac{f_o^2}{gH}\psi_1 \tag{1.23}$$

$$q_2 = \beta y + \nabla^2\psi_2 + \frac{f_o^2}{g'H}(\psi_1 - \psi_2)\,, \tag{1.24}$$

where the term $f_o^2\psi_1/gH$ is much smaller than the others and can be dropped from the equations.

Note, that we now have a closed set of equation to solve. The equations above are only dependent on ψ_1 and ψ_2, and as they are the potential vorticity for each layer, they are exactly conserved ($dq_i/dt = 0$). Nonetheless, it is convenient to nondimensionalize the variables; and we use the same scales as in ref. [13] for this purposes. That is, we use U for the characteristic velocity of the flow, $L_R = (g'H)^{1/2}/f_o$ the internal Rossby deformation radius as the horizontal scale, and L_R/U for the time scale. This way, (1.23) and (1.24) transform to:

$$q_1^* = \beta^* y + \nabla^2\psi_1^* + F(\psi_2^* - \psi_1^*) \tag{1.25}$$

$$q_2^* = \beta^* y + \nabla^2\psi_2^* + F(\psi_1^* - \psi_2^*)\,, \tag{1.26}$$

where $\beta^* = \beta U/L_R^2$ and $F = f_o^2 L_R^2/(g'H)$ [13]. The superscript denotes a nondimensional variable and will be dropped hereafter, writing above equations as:

$$q_1 = \beta y + \nabla^2\psi_1 + F(\psi_2 - \psi_1) \tag{1.27}$$

$$q_2 = \beta y + \nabla^2\psi_2 + F(\psi_1 - \psi_2) \tag{1.28}$$

[13] Sebastian: I am not really sure if these is set to one in the simulations, however it is in ref. [13]

Lastly, it is also convenient to introduce some sort of dissipation in the system. Linear drag can be added easily by considering the conservation equations for q_i as in ref. [13], that is:

$$\frac{dq_i}{dt} = \frac{\partial q_i}{\partial t} + J(\psi_i, q_i) = -\nu\nabla^2\psi_i \,, \tag{1.29}$$

where $J(\psi, q) = \psi_x q_y - \psi_y q_x$ and ν is a nondimensional viscosity coefficient. Equivalently these equations can be rewritten as:

$$\begin{aligned}
\frac{\partial}{\partial t}\left(\nabla^2\psi_1 + F(\psi_2 - \psi_1)\right) + \mathbf{u}\cdot\nabla\left(\nabla^2\psi_1 + F(\psi_2 - \psi_1)\right) + \beta\frac{\partial\psi_1}{\partial x} &= -\nu\nabla^2\psi_1 \\
\frac{\partial}{\partial t}\left(\nabla^2\psi_2 + F(\psi_1 - \psi_2)\right) + \mathbf{u}\cdot\nabla\left(\nabla^2\psi_2 + F(\psi_1 - \psi_2)\right) + \beta\frac{\partial\psi_2}{\partial x} &= -\nu\nabla^2\psi_2
\end{aligned} \tag{1.30}$$

The last two equations constitute a closed set for ψ_1 and ψ_2, far more convenient than its dimensional form, as all terms are scaled so that its magnitude is $O(1)$. We can now use this model as a simplified version to study baroclinic instability. Nonlinear terms are retained, so that its dynamics still is rich and not fully understand up to date.

1.5 Stability Theory

As we seen in the previous chapter, geostrophy is an equilibrium state of the Navier-Stokes equations. It is now convenient to ask how stable this state is, that is, how much does the isopycnals need to slope in order for baroclinic instability to develop, or equivalently, how fast the winds must be. For this we assume a background state of the flow, linearize the equations of motion around this state, assume a sinusoidal form for the disturbances and extract stability coefficients from the analysis (i.e. a bifurfication analysis is performed). It is fair to say that this has been the most common approach when dealing with baroclinic instability. And there have been great studies which differ in their assumptions. Here we focus in the particular set of equations derived in the previous sections (commonly called the Philip problem). However, more general forms of this analysis exist, where the equations for a continuously stratified atmosphere are considered (for example in the Eady or the Charney problems).

It is also important to keep in mind the limitations of this kind of analysis. They are highly idealized as they consider linearized relationships around simple background flows. Nevertheless, they are indispensable to understand atmospheric and oceanic circulation

We follow the procedure outlined by Hasha [12] or in a simpler fashion in ref. [7], as it is an elegant systematic approach which borrows notation from quantum mechanics. First, assume a shear flow with mean velocities U in the upper layer and $-U$ in the lower one. This implies that the stream functions can be computed as:

$$\begin{aligned}
\psi_1 &= -Uy + \psi_1' \\
\psi_2 &= Uy + \psi_2' \,,
\end{aligned} \tag{1.31}$$

where the primes denote perturbations around the mean state. Replacing this in (1.30), and ignoring the high order perturbation terms and viscous dissipation [14], one obtains:

$$\begin{aligned}\left(\frac{\partial}{\partial t}+U\frac{\partial}{\partial x}\right)\left(\nabla^2\psi_1+F(\psi_2-\psi_1)\right)+\frac{\partial\psi_1}{\partial x}(\beta+2FU)=0\\ \left(\frac{\partial}{\partial t}+U\frac{\partial}{\partial x}\right)\left(\nabla^2\psi_2+F(\psi_1-\psi_2)\right)+\frac{\partial\psi_2}{\partial x}(\beta-2FU)=0\end{aligned}\quad, \tag{1.32}$$

where we have dropped the primes. This can be written in matrix form as:

$$\left(\frac{\partial}{\partial t}M-L\right)\Psi=0\,, \tag{1.33}$$

where

$$\begin{pmatrix}\nabla^2-F & F\\ F & \nabla^2-F\end{pmatrix} \tag{1.34}$$

$$\begin{pmatrix}-U\frac{\partial}{\partial x}(\nabla^2-F)-(\beta+2FU)\frac{\partial}{\partial x} & -UF\frac{\partial}{\partial x}\\ UF\frac{\partial}{\partial x} & U\frac{\partial}{\partial x}(\nabla^2-F)-(\beta-2FU)\frac{\partial}{\partial x}\end{pmatrix} \tag{1.35}$$

Seeking solutions of the form

$$\Psi(x,y,t)=\hat{\Psi}(k,m,U)e^{i(kx+my-\omega t)}\,, \tag{1.36}$$

where k, m are the horizontal wave numbers and ω the frequency of the perturbation, one obtains new matrixes $\hat{M}$ and $\hat{L}$ as functions of this new variables (see ref. [12]), so that:

$$\left(\hat{L}+i\omega\hat{M}\right)\Psi=0\,. \tag{1.37}$$

In order to have nontrivial solution the determinant of $\left(\hat{L}+i\omega\hat{M}\right)$ must vanish, which gives a relation for ω (i.e. the dispersion relationship for the perturbations) and a critical velocity for the flow to be unstable. However, in our specific case we would set $\beta=0$ so that the flow would always be unstable.[15] Thinking in terms of state space for the dynamical system [16] (seeref. [14]), what was has been done up to here, is to find an equilibrium point of the system and analyze its bifurcations. This is no small task, and that is the reason of the vast amount of literature published in the subject. Now we are interested in what happens next. And we will try to analyze this by making use of the symmetries of the flow.

[14] Sebastian: I have ignored dissipation here so I think that the same results as in Vallis' should be obtained. However, notation is a bit different.

[15] Unless the domain is not wide enough for the instability to occur.

[16] That is, decomposing the PDE of the flow into a series of ODE for the amplitude of the harmonics.

1.6 Nonlinear Theory

1.6.1 A New Framework

At this point we have a good idea of what baroclinic instability is and how it has been commonly approached. Now we wish to move on and try to explore the dynamics described by our simplified model while retaining all nonlinear contributions. We will need a smart way to solve our equations of motion, and an even smarter way to represent their solutions.

The first step is to think about our equations in a dynamical framework; that is, in state space. Thus, writing the system as follows:

$$\frac{dX_i}{dt} = F(X_i) \tag{1.38}$$

where each X_i correspond to a coordinate in this space. Clearly, not the case of (1.4), where $\mathbf{u}$ is a dependent variable of both space and time. Nonetheless, we can formulate it in this form by the use of spectral methods expressing the velocity as:

$$\mathbf{u} = \sum \widehat{u}\phi(\mathbf{x}) \tag{1.39}$$

where ϕ are basis function defined for the entire domain[17] and $\widehat{u}$ their respective amplitudes. Substituting this in (1.6), and using and appropriate relationship to account for the pressure, we obtain a system like (1.38) for the amplitudes of the basis functions. That is:

$$\frac{d\widehat{u}_i}{dt} = G(\widehat{u}_i) \tag{1.40}$$

system which can be relatively easily integrated. [18] It should be noted that the above is much more than just a convenient method to solve the Navier-Stokes equations; it is a framework to study continuum equations as dynamical systems. In state space, a point represents a physical state of the full system, i.e. the three dimensional velocity field. This implies that Navier-Stokes equations can be thought as an infinite dimensional space where the harmonics represent each dimension of it [19]. However, the number of dimension consider in practice is finite and limited either by the computer power available, or the smallest scale one can actually solve. No long time ago considering only a handful of dimensions was possible. Nowadays, computer power is such that DNS[20] are possible and considering 100,000 dimensions or more is common for small domains.

But given the exuberant number of dimensions, how are we to visualize the flows in state space? there is not need to panic about this, although visualizations is challenging the important dynamics are embedded in lower dimensional manifolds. This was first

[17] This could be any set of orthogonal functions (i.e. Fourier, Legendre or Chebyshev series)

[18] Predrag: will believe it when I see the results

[19] This view is due to Hopf, who's insight on turbulence where way ahead of his time; and have proven to be an invaluable tool (see ref. [15])

[20] Direct Numerical Simulations. The approach of this method is to solve Navier-Stoke equations up to the scale where dissipation occurs and kinetic energy is converted to heat.

noted by Hopf, who speculated that viscosity must lower the effective dimensions of the system. An example would be a laminar flow which is embedded in a infinite space; which due to its high viscosity is effectively represented by a single point in this space (for instance see ref. [3]). In the case of a turbulent flow invariant solutions (periodic orbits, relative periodic orbits, equilibrium points and traveling waves) are starting point for finding the lower dimensional invariant manifolds to consider. These solutions are usually unstable, which makes imperative the use of a search algorithm in order to find them.

Nonetheless, their role in dynamics is of such importance (see ref. [16]) that these intrinsic difficulties should not discourage us from seeking for them. For instance, invariant solutions can be thought to represent the coherent structures that characterize turbulent dynamics (see refs. [17, 18]). In this view, the system spends some time in a neighbor near one of this solutions, then jumps to the next and spends some time there until it jumps to another, and so on. What it is most striking is that this cycles resemble closely turbulent trajectories, and are hard to tell apart from them. In fact, the measurable quantities of a system depend mostly on these invariant solutions (see ref. [14]), so that finding them gives a better understanding of the system. In this study we give the first steps towards finding these solutions in a baroclinic instability model by showing a plausible way to reduce the symmetries of the system.

Reducing the symmetries greatly simplifies the search of this structures. As solution do not wonder as much in the reduced state space. In this space, traveling waves reduce to equilibrium points, relative periodic orbits to periodic orbits and equilibrium points are conserved. Our tool of choice for this reduction is the method of slices. We are interested in rotating all the solutions to a hyperplane which intersects all symmetry group tangents (see ref. [14] for details). For this we impose the condition:

$$\frac{\partial}{\partial \phi} \| a - g\hat{a}' \|^2 = 0 \,, \tag{1.41}$$

where a is our vector in state space, ϕ the rotating frame (i.e. the angle by which the solution is rotated) and $\hat{a}'$ a template representative of our local dynamics. Of course, our slice would not be good for the entire manifold, and it is necessary to consider a set of this slices in order to capture the entire dynamics of the system ref. [19]. More details of this will be given in the next section.

Once we are done with the slicing, the hope is that this makes it easier to look for this invariant solutions. After all, the "dancing" solutions have been settled to the slice. But first, we need to define them in a quantitative manner so it is clear what we mean by invariant solutions. First, let's think again in terms of physical space (1.6). Note that we can write the system as:

$$\frac{\partial \mathbf{u}}{\partial t} = F(\mathbf{u}) \,, \quad f^t(\mathbf{u}) = \mathbf{u} + \int_0^t F(\mathbf{u}) d\tau \,, \tag{1.42}$$

thus, we are seeking solutions of the following form (as shown in ref. [3]):

$$\begin{aligned} F(\mathbf{u}_{EQ}) &= 0 \\ F(\mathbf{u}_{TW}) &= -c \cdot \nabla \mathbf{u}_{TW} \\ f^{T_p}(\mathbf{u}_p) &= u_p \\ f^{T_p}(\mathbf{u}_p) &= u_p \,, \end{aligned} \tag{1.43}$$

[21] where this represent respectively equilibrium points, relative equilibrium points, periodic orbits and relative periodic orbits.

Finally, note that one additionally aspect one should care about is the connection between these different solutions. That is, how is one to get from one recurrent pattern to the other? Heteroclitic connections (i.e. the trajectories which exactly connect invariant solutions; see for instance ref. [20]), are commonly studied for this purposes as these organize how the flow transits from one manifold to the next.

In this project, we limit ourselves to show how to make the slicing, hoping this would encourage more in depth study of the subject. However, we briefly discuss next how to start searching for the recurrences in the system one the slicing is completed.

1.6.2 Finding invariant solutions

Finding invariant solution of a system with a high number of dimension is not an easy task. And it is even harder if we do not reduce the symmetries first. In doing so one is required to use a numerical method to find them. However, due to the fact that huge Jacobian matrix would have to be computed, implementing the Newton-Raphson standard search method is not an option.

But not all hope is lost. Algorithms to find this structures have been implemented and used successfully in a variety of simulations[22] (see for instance ref. [18]). This methods depend on initial guesses of this periodic orbits, and there are several approaches one can take to make the right ones. One of this approaches is given in ref. [18], where the rate of energy dissipation and energy input for a system is computed based on the velocity field, and then plotted together. This way the entire multidimensional system is projected into two physical meaningful dimensions and guesses are made based on approximate recurrences of the traced curve. [23]

After reducing the symmetries, the next step would be to evaluate the possibility of a periodic orbit based on the criteria discussed here. However, we proceed one step at a time. So let us go back to reducing the symmetry.

1.6.3 Symmetry Reduction

Up to here we have gather enough background to start making attempts to reduce the symmetry. The system to consider is that of Section 1.4. And the code is the same as

[21] Sebastian: I have to fix the second equation justification.
[22] Sebastian: Insert references in the future)
[23] Sebastian: FIGURE I will put her one of the figures of Viswanath's paper

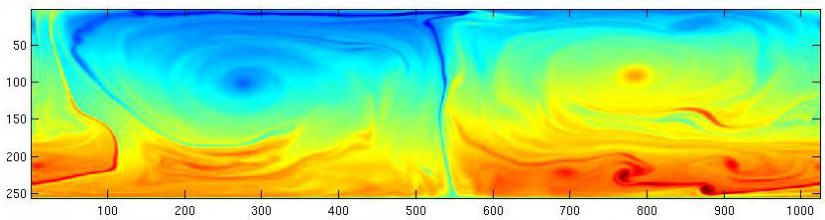

Figure 1.5: Vorticity field (ξ) for the top layer in the model.

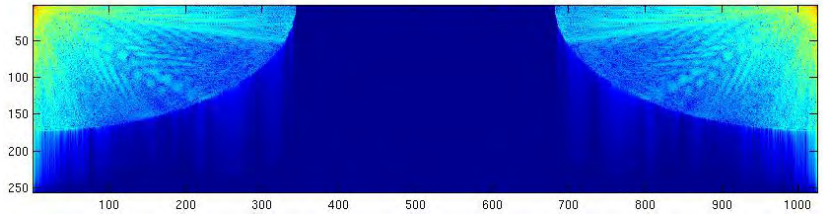

Figure 1.6: Spectral representation of the vorticity field ($ln(1 + abs(a_{lk}))$). Note that some frequencies are just the complex conjugate of others.

the one programmed by Bracco in ref. [13][24]. The typical results of the simulation are shown in figure 1.6.

The code makes uses a pseudo-spectral method to solve the nonlinear PDE given in 1.32 but with $\beta = 0$ and $\psi_2 = \psi_2'$. For this, Fast Sine Transforms are used along the y direction, and Fast Fourier Transforms along the x direction . This means that the vorticity can be represented as:

$$\xi(x, y) = \sum_{k=0}^{N-1} a_{lk} e^{-2i\pi kx/N} \tag{1.44}$$

Additionally, the system has periodic boundaries along the x axis, so it has a continuous symmetry along this axis $\xi(x) = \xi(x + L_x)$; where L_x stands for the length of the domain. The one-parameter rotation group acting on this variable, would be then given by (see ref. [4]):

$$g(\phi) = \text{diag}\{e^{-2i\pi k\phi/N}\} \tag{1.45}$$

When acting on a point in state space ($g(\phi)a$), the effect of g is to translate the solution along x without changing any o the properties of the simulation. Furthermore, in state space the group orbit traces a trajectory which topologically is a circle, and the group tangent of the circle at point a is given by the derivative of g:

$$\mathbf{T} = \text{diag}\{-2i\pi k/N\} \tag{1.46}$$

[24] Without bottom topography or beta effect.

Now, to reduce the symmetry, we select a template representative our our physical simulation (the slice a'), and seek for the rotating frame $\phi(t)$ that continually rotates a trajectory back to the slice. This, by making use of condition 1.41. Care is taken as we are dealing with complex vectors, so that the norm represents the multiplication of a vector with its conjugate transform. That is, starting with:

$$\frac{\partial}{\partial\phi} \| a - g\hat{a}' \|^2 = 0 \,, \tag{1.47}$$

expanding, simplifying and noting that $\mathrm{Re}\,(a^\dagger \mathbf{T} a) = 0$ one arrives at the slicing condition:

$$\mathrm{Re}\,(\hat{a}^\dagger \mathbf{T} \hat{a}') = 0 \tag{1.48}$$

which is a similar condition to the one obtained for real cases. Translating it into a somewhat more implementable equation gives:

$$\mathrm{Re}\,(\hat{a}^\dagger \mathbf{T} \hat{a}') = \mathrm{Re}\left(\frac{-2\pi i}{N} \sum_{k=0}^{N-1} \sum_{k=0}^{M-1} \overline{a_{lk}} a'_{lk} k e^{\frac{-2\pi i k}{N}\phi} \right) = 0 \tag{1.49}$$

Now we are all set to seek for this solutions. A Newton-Raphson, or similar, seeking method can be implemented by using $F(\phi) = \mathrm{Re}\,(\hat{a}^\dagger \mathbf{T} \hat{a}')$ and $F'(\phi) = \frac{\partial}{\partial\phi}\mathrm{Re}\,(\hat{a}^\dagger \mathbf{T} \hat{a}')$ for each time step. Effort are being carried right now to implement this algorithm, however for the time being we only provide the methodology.

[25] The template $\hat{a}'$ should be a generic state space point in the sense that its group orbit has the full dimension of the group G. The set of the group orbit points closest to the template $\hat{a}'$ forms a neighborhood of $\hat{a}'$ in which each group orbit intersects the hyperplane *only once*. A slice hyperplane captures neighboring group orbits until, for a point $\hat{a}^*$ not so close to the template, the group tangent vector $t(\hat{a}^*)$ lies in the slice hyperplane. The group orbits for such points are grazed tangentially rather than sliced transversally, much like what happens at the section border for evolution in time. This is also a linear condition and defines the chart border $\mathcal{S}$, [21, 22] a $(d-2)$-dimensional manifold, which contains all the points $\hat{a}^*$ whose group tangents lie in the slice hyperplane, i.e.,

$$\langle \hat{a}^* | t' \rangle \;=\; 0 \text{ and } \langle t(\hat{a}^*) | t' \rangle \;=\; 0 \,. \tag{1.50}$$

$\mathcal{S}$ also contains all points for which $t(\hat{a}^*) = 0$. While for the Poincaré sections the analogous points were equilibria (captured only if the section cut through them), for slice hyperplanes points with vanishing group actions belong to invariant subspaces, and, by its definition, every chart border automatically includes *all* invariant subspaces.

The norm square of a tangent vector is given by

$$\|t(a)\|^2 = -\langle t(a) | t(a) \rangle = \frac{2\pi}{N} \sum_{k=0}^{N-1} \sum_{k=0}^{M-1} k^2 \, \overline{a_{lk}} a_{lk} \,. \tag{1.51}$$

[25] Predrag: insert from Chaos Gang paper, rewrite

The product of the two tangents in (1.49) is weighted by the SO(2) quadratic Casimir [26]

$$-\mathrm{Re}\,(\hat{a}^\dagger \mathbf{T}^2 \hat{a}') = \mathrm{Re}\left(\frac{-2\pi i}{N}\sum_{k=0}^{N-1}\sum_{k=0}^{M-1}\overline{a_{lk}}a'_{lk}k^2 e^{\frac{-2\pi i k}{N}\phi}\right). \tag{1.52}$$

1.7 Acknowledgments

The author would like to acknowledge the valuable discussions and advice obtained during the course of the semester from Professors Predrag Cvitanović, Annalisa Bracco and Peter J. Webster, as well as the students and researchers that attended the Spring 2012 "PHY-7224 Nonlinear Dynamics". This was a very enjoyable and enlightening experience.

[26] Predrag: I have not checked (1.49), (1.51) and/or (1.52)

Bibliography

[1] B. Hof *et al.*, Experimental observation of nonlinear traveling waves in turbulent pipe flow, Science **305**, 1594 (2004).

[2] F. Waleffe, On a Self-Sustaining Process in shear flows, Phys. Fluids **9**, 883 (1997).

[3] J. F. Gibson, J. Halcrow, and P. Cvitanović, Visualizing the geometry of state-space in plane Couette flow, J. Fluid Mech. **611**, 107 (2008).

[4] A. P. Willis, P. Cvitanović, and M. Avila, Revealing the state space of turbulent pipe flow by symmetry reduction, J. Fluid Mech. **721**, 514 (2013).

[5] A. E. Gill, *Atmosphere-ocean dynamics* (Academic, London, 1982).

[6] J. R. Holton, *An introduction to dynamic meteorology* (Academic, New York, 1979).

[7] R. Salmon, *Lectures on Geophysical Fluid Dynamics* (Oxford Univ. Press, Oxford, 1998).

[8] P. K. Kundu and I. Cohen, *Fluid Mechanics* (Academic, San Diego, CA, 2008).

[9] G. K. Vallis, *Atmospheric and Oceanic Fluid Dynamics: Fundamentals and Large-scale Circulation* (Cambridge Univ. Press, Cambridge, 2006).

[10] N. A. Phillips, A simple three-dimensional model for the study of large-scale extratropical flow patterns, J. Meteorology **8**, 381 (1951).

[11] A. Majda, *Introduction to PDEs and Waves for the Atmosphere and Ocean* (American Mathematical Society, New York, 2003).

[12] A. E. Hasha, A search for baroclinic structures, Proceed. 2005 WHOI Summer. Geophysical Fluid Dynamics Program (2005).

[13] A. Bracco and J. Pedlosky, Vortex generation by topography in locally unstable baroclinic flows, J. Phys. Oceanogr. **33**, 207 (2003).

[14] P. Cvitanović, R. Artuso, R. Mainieri, G. Tanner, and G. Vattay, *Chaos: Classical and Quantum* (Niels Bohr Inst., Copenhagen, 2022), https://ChaosBook.org.

[15] E. Hopf, A mathematical example displaying features of turbulence, Commun. Pure Appl. Math. **1**, 303 (1948).

[16] P. Cvitanović, Periodic orbits as the skeleton of classical and quantum chaos, Physica D **51**, 138 (1991).

[17] F. Christiansen, P. Cvitanović, and V. Putkaradze, Hopf's last hope: Spatiotemporal chaos in terms of unstable recurrent patterns, Nonlinearity **10**, 55 (1997).

[18] D. Viswanath, Recurrent motions within plane Couette turbulence, J. Fluid Mech. **580**, 339 (2007).

[19] P. Cvitanović, D. Borrero-Echeverry, K. Carroll, B. Robbins, and E. Siminos, Cartography of high-dimensional flows: A visual guide to sections and slices, Chaos **22**, 047506 (2012).

[20] J. Halcrow, J. F. Gibson, P. Cvitanović, and D. Viswanath, Heteroclinic connections in plane Couette flow, J. Fluid Mech. **621**, 365 (2009).

[21] E. Siminos and P. Cvitanović, Continuous symmetry reduction and return maps for high-dimensional flows, Physica D **240**, 187 (2011).

[22] S. Froehlich and P. Cvitanović, Reduction of continuous symmetries of chaotic flows by the method of slices, Commun. Nonlinear Sci. Numer. Simul. **17**, 2074 (2012).

[23] J. E. Hart, Finite amplitude baroclinic instability, Ann. Rev. Fluid Mech. **11**, 147 (1979).

[24] W. R. Young, Selective decay of enstrophy and the excitation of barotropic waves in a channel, J. Atmos. Sci. **44**, 2804 (1987).

[25] J. von Hardenberg, K. Fraedrich, F. Lunkeit, and A. Provenzale, Transient chaotic mixing during a baroclinic life cycle, Chaos **10**, 122 (2000).

[26] J. Hamilton, J. Kim, and F. Waleffe, Regeneration mechanisms of near-wall turbulence structures, J. Fluid Mech. **287**, 317 (1995).

[27] D. Tempelmann, A. Hanifi, and D. S. Henningson, Spatial optimal growth in three-dimensional boundary layers, J. Fluid Mech. **646**, 5 (2010).

[28] M. Lombardi, C. Caulfield, C. Cossu, A. Pesci, and R. Goldstein, Growth and instability of a laminar plume in a strongly stratified environment, J. Fluid Mech. **671**, 184 (2011).

[29] G. Kawahara and S. Kida, Periodic motion embedded in plane Couette turbulence: Regeneration cycle and burst, J. Fluid Mech. **449**, 291 (2001).

[30] J. M. Greene and J.-S. Kim, The steady states of the Kuramoto-Sivashinsky equation, Physica D **33**, 99 (1988).

[31] P. Cvitanović, R. L. Davidchack, and E. Siminos, On the state space geometry of the Kuramoto-Sivashinsky flow in a periodic domain, SIAM J. Appl. Dyn. Syst. **9**, 1 (2010).

[32] U. Frisch, *Turbulence* (Cambridge Univ. Press, Cambridge, 1996).

[33] G. D. Mostow, Equivariant embeddings in Euclidean space, Ann. Math. **65**, 432 (1957).

[34] R. S. Palais, On the existence of slices for actions of non-compact Lie groups, Ann. Math. **73**, 295 (1961).

[35] V. Guillemin and S. Sternberg, *Symplectic Techniques in Physics* (Cambridge Univ. Press, Cambridge, 1990).

[36] M. Golubitsky, I. Stewart, and D. G. Schaeffer, *Singularities and Groups in Bifurcation Theory* Vol. 2 (Springer, New York, 1988).

[37] C. L. Wolfe and R. M. Samelson, An efficient method for recovering Lyapunov vectors from singular vectors, Tellus A **59**, 355 (2007).

[38] R. L. Panetta and I. M. Held, Baroclinic eddy fluxes in a one-dimensional model of quasi-geostrophic turbulence, J. Atmos. Sci. **45**, 3354 (1988).

[39] R. L. Panetta, Zonal jets in wide baroclinically unstable regions: Persistence and scale selection, J. Atmos. Sci. **50**, 2073 (1993).

[40] P. Klein and J. Pedlosky, A numerical study of baroclinic instability at large super-criticality, J. Atmos. Sci. **43**, 1243 (1986).

[41] I. M. Held, R. L. Panetta, and R. T. Pierrehumbert, Stationary external Rossby waves in vertical shear, J. Atmos. Sci. **42**, 865 (1985).

[42] I. M. Held, R. T. Pierrehumbert, and R. L. Panetta, Dissipative destabilization of external Rossby waves, J. Atmos. Sci. **43**, 388 (1986).

[43] R. L. Panetta, I. M. Held, and R. T. Pierrehumbert, External Rossby waves in the two-layer model, J. Atmos. Sci. **44**, 2924 (1987).

[44] X. Zeng, R. A. Pielke, and R. Eykholt, Chaos theory and its applications to the atmosphere, Bull. Amer. Meteor. Soc. **74**, 631 (1993).

[45] I. M. Held and V. D. Larichev, A scaling theory for horizontally homogeneous, baroclinically unstable flow on a Beta plane, J. Atmos. Sci. **53**, 946 (1996).

[46] K. A. Montgomery, M. Silber, and S. A. Solla, Amplification in the auditory periphery: The effect of coupling tuning mechanisms, Phys. Rev. E **75**, 051924 (2007).

[47] D. D. Holm and B. A. Wingate, Baroclinic instabilities of the two-layer quasi-geostrophic Alpha model, J. Phys. Oceanogr. **35**, 1287 (2005).

[48] W. Weimer and H. Haken, Chaotic behavior and subcritical formation of flow patterns of baroclinic waves for finite dissipation, J. Atmos. Sci. **46**, 1207 (1989).

[49] M. Mak, Dissipative structure of a nonlinear baroclinic system: Effect of asymmetric friction, J. Atmos. Sci. **44**, 2613 (1987).

[50] P. Riviére and P. Klein, Effects of an asymmetric friction on the nonlinear equilibration of a baroclinic system, J. Atmos. Sci. **54**, 1610 (1997).

[51] T. G. Shepherd, Nonlinear saturation of baroclinic instability. Part I: The two-layer model, J. Atmos. Sci. **45**, 2014 (1988).

[52] J. Pedlosky and P. Klein, The nonlinear dynamics of slightly supercritical baroclinic jets, J. Atmos. Sci. **48**, 1276 (1991).

[53] P. Klein and J. Pedlosky, The role of dissipation mechanisms in the nonlinear dynamics of unstable baroclinic waves, J. Atmos. Sci. **49**, 29 (1992).

[54] H. Weng and A. Barcilon, Wavenumber selection for single-wave steady states in a nonlinear baroclinic system, J. Atmos. Sci. **45**, 1039 (1988).

[55] J. Pedlosky and L. M. Polvani, Wave-wave interaction of unstable baroclinic waves, J. Atmos. Sci. **44**, 631 (1987).

[56] P. Boccotti, *Wave Mechanics for Ocean Engineering* (Elsevier, New York, 2000).

[57] P. Boccotti, Field verification of quasi-determinism theory for wind waves in the space-time domain, Ocean Eng. **38**, 1503 (2011).

[58] P. Cvitanović and B. Eckhardt, Symmetry decomposition of chaotic dynamics, Nonlinearity **6**, 277 (1993).

[59] J. F. Gibson, J. Halcrow, and P. Cvitanović, Equilibrium and traveling-wave solutions of plane Couette flow, J. Fluid Mech. **638**, 243 (2009).

[60] D. A. Kopriva, *Implementing Spectral Methods for Partial Differential Equations* (Springer, New York, 2009).

[61] B. C. Hall, *Lie Groups, Lie Algebras, and Representations* (Springer, New York, 2003).

[62] S. Ortega Arango, Towards reducing continuous symmetry of baroclinic flows, in *ChaosBook.org/projects*, Georgia Inst. of Technology, 2012, https://ChaosBook.org/projects/index.shtml#Ortega.

[63] S. N. Stechmann, A. J. Majda, and B. Khouider, Nonlinear dynamics of hydrostatic internal gravity waves, Theor. Comput. Fluid Dyn. **22**, 407 (2008).

[64] A. J. Majda and S. N. Stechmann, Nonlinear dynamics and regional variations in the MJO skeleton, J. Atmos. Sci. **68**, 3053 (2011).

[65] E. Kazantsev, Unstable periodic orbits and attractor of the barotropic ocean model, Nonlin. Proc. Geophys. **5**, 193 (1998).

[66] A. S. Gritsun, Unstable periodic trajectories of a barotropic model of the atmosphere, Russian J. Numer. Analysis and Math. Modelling **23**, 345 (2008).

[67] A. Gritsun, Statistical characteristics of barotropic atmospeheric system and its unstable periodic solutions, Dokl. Earth Sciences **435**, 1688 (2010).

[68] A. Gritsun, Connection of periodic orbits and variability patterns of circulation for the barotropic model of atmospheric dynamics, Dokl. Earth Sciences **438**, 636 (2011).

[69] F. M. Selten and G. Branstator, Preferred regime transition routes and evidence for an unstable periodic orbit in a baroclinic model, J. Atmos. Sci. **61**, 2267 (2004).

[70] A. Gritsun, G. Branstator, and A. Majda, Climate response of linear and quadratic functionals using the fluctuation-dissipation theorem, J. Atmos. Sci. **65**, 2824 (2008).

[71] M. Hairer and A. J. Majda, A simple framework to justify linear response theory, Nonlinearity **23**, 909 (2010).

[72] R. V. Abramov and A. J. Majda, New approximations and tests of linear fluctuation-response for chaotic nonlinear forced-dissipative dynamical systems, J. Nonlin. Sci. **18**, 303 (2008).

[73] R. V. Abramov, Short-time linear response with reduced-rank tangent map, Chin. Ann. Math. **30**, 447 (2009).

[74] A. Gritsun, Statistical characteristics, circulation regimes and unstable periodic orbits of a barotropic atmospheric model, Philos. Trans. Royal Soc. A **371** (2013).

[75] R. Chattopadhyay, A. K. Sahai, and B. N. Goswami, Objective identification of nonlinear convectively coupled phases of monsoon intraseasonal oscillation: implications for prediction, **65**, 1549 (2008).

Chapter 2

Predrag's notes

2.1 Introduction

[1] The baroclinity (baroclinicity) of a stratified fluid is a measure of how misaligned the gradient of pressure is from the gradient of density in a fluid, proportional to the baroclinic vector

$$\frac{1}{\rho^2}\nabla\rho\times\nabla p\,, \tag{2.1}$$

which in turn is is proportional to sine of the angle between surfaces of constant pressure (isobaric surfaces) and surfaces of constant density (isopycnic surfaces). Thus, in a *barotropic* fluid (which is defined by zero baroclinity), these surfaces are parallel.

When the baroclinic vector is nonzero, the sense of the baroclinic vector is to create vorticity to make the interface level out. In the process, the interface overshoots, and the result is an oscillation which is an internal gravity wave. The energy source for baroclinic instability is the potential energy in the environmental flow. As the instability grows, the center of mass of the fluid is lowered. Baroclinic flows can be contrasted with barotropic flows in which density and pressure surfaces coincide and there is no baroclinic generation of vorticity. 'Baroclinic' means that the instability is driven by density difference; 'barotropic' means not.

Beginning with the equation of motion for a fluid and taking the curl, one arrives at the equation of motion for the curl of the fluid velocity, i.e. the vorticity. In a fluid that is not all of the same density, a source term appears in the vorticity equation whenever surfaces of constant density and surfaces of constant pressure are not aligned. The material derivative of the local vorticity is given by

$$\frac{D\vec{\omega}}{Dt}\equiv\frac{\partial\vec{\omega}}{\partial t}+(\vec{u}\cdot\vec{\nabla})\vec{\omega}=(\vec{\omega}\cdot\vec{\nabla})\vec{u}-\vec{\omega}(\vec{\nabla}\cdot\vec{u})+\underbrace{\frac{1}{\rho^2}\vec{\nabla}\rho\times\vec{\nabla}p}_{\text{baroclinic contribution}}\quad, \tag{2.2}$$

where $\vec{u}$ is the velocity and $\vec{\omega}$ is the vorticity, p is pressure, and ρ is density). The baroclinic vector (2.1) is of interest both in compressible fluids and in incompressible

[1] Predrag: the text here is taken from en.wikipedia.org/wiki/Baroclinic, needs to be rewritten

(but inhomogenous) fluids. Internal gravity waves as well as unstable Rayleigh-Taylor modes can be analyzed from the perspective of the baroclinic vector. It is also of interest in the creation of vorticity by the passage of shocks through inhomogenous media, such as in the Richtmeyer-Meshkov instability.

Baroclinic instability arises in rapidly rotating, strongly stratified fluids. [2] Baroclinic instability occurs when vertical shear flows driven by horizontal temperature gradients in a rotating domain become unstable, and large, wavelike disturbances develop that redistribute temperature fields in a kind of horizontally slanted convection. Whether a fluid counts as rapidly rotating is determined by the *Rossby number*, a measure of how close the flow is to solid body rotation. A flow in solid body rotation has vorticity that is proportional to its angular velocity. The Rossby number is a measure of the departure of the vorticity from that of solid body rotation. The Rossby number must be small for the concept of baroclinic instability to be relevant. [3]

The term "baroclinic" refers to the mechanism by which vorticity is generated. Vorticity is the curl of the velocity field. The evolution of vorticity can be broken into contributions from advection (as vortex tubes move with the flow), stretching and twisting (as vortex tubes are pulled or twisted by the flow) and baroclinic vorticity generation, which occurs whenever there is a density gradient along surfaces of constant pressure.

The simplest example of a stably stratified flow is an incompressible flow with density decreasing with height. One measures the strength of the stratification by asking how large the vertical shear of the horizontal winds has to be in order to destabilize the flow and produce the classic Kelvin-Helmholtz instability. This measure is the Richardson number. When the Richardson number is large, the stratification is strong enough to prevent this shear instability.

The most geophysically relevant case is a channel whose zonal length is substantially greater than its meridional breadth. In this instance the form of the minimum enstrophy solution is decided by the ratio of the energy to the squared momentum. When this parameter is below a critical value one has a parallel flow, while if this value is exceeded, the minimum enstrophy solution is a Rossby wave. Periodic boundary conditions are physically motivated for a model of atmospheric dynamics, because the mid-latitude β-plane is typically conceived as a periodic strip wrapping around the earth. A typical wavelength for a baroclinic disturbance in the atmosphere is about 2000 km, which leaves space for only ten to fifteen wave periods in a complete traversal of the globe at mid-latitudes. Nonetheless, there are physical examples of baroclinic instability to which the large aspect ratio approximation is applicable. For example, baroclinic instability produces eddies in ocean currents on the scale of 200 km. In an ocean measuring several thousand kilometers across, there is plenty of room for large scale structures to emerge.

[4] A number of models have been used to study this phenomenon, the most well known of which are the Charney model and the Eady model. A basic introduction to these models and others can be found in the textbooks by Pedlosky [9], and Gill [4].

[2] Predrag: the sentence taken from Woods Hole, *A Search for Baroclinic Structures* by Alexander E. Hasha (2005), ref. [12] needs to be rewritten.

[3] Predrag: maybe read ref. [23, 24, 25]? this one might be just simple enough for me - it's highschool level.

[4] Predrag: the text here is taken from Woods Hole, Hasha report, needs to be rewritten

In this analysis, we use perhaps the simplest model exhibiting baroclinic instability. Introduced by Phillips in 1954 [10], it consists of a two-layer quasi-geostrophic flow in a rotating channel. Phillips analyzed the linear stability of a shear flow in which the fluid in each layer moves with a uniform zonal velocity. The basic state differs from that of the standard Kelvin-Helmholtz instability because rotation forces a slanting of the free surface between the two layers in order to balance the Coriolis force on the zonal flow. Phillips found that instability occurs when the difference between the velocities of the two layers exceeds a critical threshold. The model can easily be modified to include important physical effects, such as dissipation or a planetary vorticity gradient.

In this work, the baroclinic instability is modeled by a 2-layer incompressible viscous fluid in a channel with no-slip side walls, periodic in streamwise direction, top layer driven by 'atmospheric stream', i.e. a constant total streamwise volume flow per unit time. We simply impose uniform streamwise velocity of unit size, ignoring the boundary condition (could use a parabolic profile). With free slip the layers are still unstable in the same way, just the boundary behavior is different. Oceanographers prefer no-slip, perhaps because of coastal stream. The bottom layer is not forced, no slip, no Ekman layer (Ekman layer models friction at the bottom; that would make sense when one works with 50 layers, but not two). The two layers are coupled by the difference $\Phi_2 - \Phi_1$. Laplacian of stream function is vorticity. Each layer is computed in terms of vorticity equations as a 2-dimensional fluid. The lower layer has higher fluid density, and they are coupled across their interface by difference of vorticity.

In our simulation this is about factor two; it is related to the Rösby deformation radius L_R. The spanwise y width is $L_R/2\pi = 1/2$. Unless the width is larger than L_R, no instability. The stream-wise aspect ration is about 8.

The present work is motivated by a series of papers by Pedlosky ([6], [7], and a paper by Romea [11] that analyzed the nonlinear development of baroclinic instability in the Phillips model in a number of physically interesting situations. Pedlosky's papers, in particular, were the first to use multiscale asymptotic methods to compute amplitude equations for baroclinic instability. In contrast to the present effort, Pedlosky and Romea used periodic zonal boundary conditions and were therefore investigating the nonlinear interaction of a discrete spectrum of unstable modes. Consequently, their calculation led to amplitude ODEs as described above.

Our analysis of the large aspect ratio Phillips model should provide some insight into the kinds of structures one might expect in these situations.

[5] The flow to be considered is that of N layers of $2D$ incompressible viscous fluid confined within a rectangular channel, driven by a mean unit velocity added to the top layer in the stream-wised direction. The Reynolds number is defined as $Re = ?UL/\nu?$, where U is the mean velocity??? of the flow, L is the channel span-wise width, and ν is the kinematic viscosity. We scale lengths by $L/2$ and velocities by $2U$ in the Navier-Stokes equation (2.2) for $\vec{u}$, the deviation from the laminar flow equilibrium $U(r) = 1 - r^2$. Here the dimensionless variable β is the fractional pressure gradient, additional to the laminar flow, required to maintain a constant mean velocity U. A Reynolds number Re_p, based on the applied pressure gradient, is given by $Re_p = ??$, whereas the friction Reynolds number is $Re_t = ??$. The Navier-Stokes equation are

[5] Predrag: the text here is taken from the pipes/slice article, needs to be rewritten

formulated in cylindrical-polar coordinates, where (x, y, n) are the stream-wise, span-wise positions and layer, respectively. The full fluid velocity field $U(r)\hat{\mathbf{z}} + \vec{u}$ is represented by $[u, v, w, p](r, \theta, z)$, with u, v and w respectively the radial, azimuthal and stream-wise velocity components, and p the pressure. In numerical simulations no-slip boundary conditions are imposed at the side walls and periodic boundary conditions in the stream-wise x direction. The computational domain is

$$\Omega = (x, y, n) \in [0, 2\pi/\alpha] \times [0, 2] \times [n]\,,$$

where $L = 2\pi/\alpha$ is the length of the domain.

This study is conducted at *Re* =??, with $N = 2$ and $\alpha = 1.25$, corresponding to a short $L \simeq 4 \times 2$-periodic cell in the stream-wise direction,

$$\Omega \ = [1, \pi, 2\pi/1.25] \qquad \approx [90, 283, 452] \quad \text{wall units} \tag{2.3}$$

At *Re* =?? this computational cell empirically sustains turbulence for very long times. In average the additional pressure fraction required to support turbulence while keeping constant mass-flux is $\langle\beta\rangle_t = 0.70$, yielding friction Reynolds number $Re_t = 90.3$. At this Reynolds number and geometry one domain width 2 corresponds to about 90? wall units. The domain size (2.3) was chosen as a compromise between the computational preference for small domains *vs.* the need for the domain to be sufficiently long to accommodate turbulent dynamics. In addition, restricting the largest wavelength is very useful in identifying key coherent structures characterizing turbulent dynamics [26]. Although the cells studied in this paper are short, the two-dimensional states explored here by equilibria and their unstable manifolds are strikingly similar to typical states in longer domains.

A choice of a basis set for function space of solutions is greatly aided by the symmetries of the flow. Baroclinic domains are stream-wise (in numerical work) periodic, so deviation velocity field $\vec{u}$ and deviation pressure in the Navier-Stokes equations (2.2) are expanded in Fourier modes in the stream-wise and span-wise directions,

$$\vec{u}(x, y, n) = \sum_{|k|<K} \sum_{|m|<M} \vec{u}_{nkm}\, \mathrm{e}^{\mathrm{i}(\alpha x z + m y)}\,, \tag{2.4}$$

whereas N layers are used in the vertical direction. Flow states are typically characterized by the instantaneous kinetic energy of their deviation from laminar flow, $E = \frac{1}{2}\|\vec{u}\|^2$, and energy dissipation rate $D = 1/Re\|\nabla \times \vec{u}\|^2$. The dissipation rate is balanced by the energy fed into the flow as

$$\dot{E} = I - D\,, \tag{2.5}$$

where $I = \oint dS\,(\mathbf{n} \cdot \vec{u})\, p$ is the additional instantaneous external power required to maintain constant flux, over that of the laminar flow. For relative equilibria the kinetic energy is constant and so $D = I$, such solutions sit on the diagonal in figure **??**, whereas for relative periodic orbits the kinetic energy is time-periodic, with $\overline{D} = \overline{I}$ only for long-time averages. [6]

[6] Predrag: It would be instructive to supplement (I, E), by the (I, D) plot as well

2.2 Energy, dissipation, etc.

2012-03-27 PC In rev. 2294 moved this to `siminos/baroclinic/PCnotes.tex`, there to persuade Annalisa and Sebastian to plot some state space invariants cheaply.

2013-03-31 PC Annalisa and Sebastian showed no interest, so the text is back in `siminos/blog/energy.tex`.

2.2.1 State-space visualization of fluid flows

Hopf [15] envisioned the function space of Navier-Stokes velocity fields as an infinite-dimensional state space $\mathcal{M}$ in which each instantaneous state of $3D$ fluid velocity field $\mathbf{u}(\mathbf{x})$ is represented as a unique point a. In our particular application we can represent $a = (\vec{u}_{nkm})$ as a vector whose elements are the primitive discretization variables (2.4). The $3D$ velocity field given by $\vec{u}_{knm}(t)$, obtained from integration of the Navier-Stokes equations in time, can hence be seen as trajectory $a(t)$ in $\approx 100,000$ dimensional space spanned by the free variables of our numerical discretization, with the Navier-Stokes equation (2.2) (or Kuramoto-Sivashinsky equation) rewritten as

$$\dot{a} = F(a), \qquad a(t) = a(0) + \int_0^t \mathrm{d}t'\, F(a(t'))\,, \tag{2.6}$$

where the current state of the fluid $a(t)$ is the time-t forward map of the initial fluid state $a(0)$.

In order to quantify whether two fluid states are close or far from each other, one needs a notion of distance between two points in state space, measured here as

$$\|a - a'\|^2 = \langle a - a' | a - a' \rangle = \int_\Omega d\mathbf{x}\, (\vec{u} - \vec{u}') \cdot (\vec{u} - \vec{u}')\,. \tag{2.7}$$

As there is no compelling reason to use this 'energy norm', other than that velocity fields is what is given in a numerical computation, what norm one uses depends very much on the application. In the study of 'optimal perturbations' that move a laminar solution to a turbulent one, both energy [27] and dissipation [28] norms have been used. In our searches for relative equilibria and relative periodic orbits we find it advantageous to use a 'compensatory' norm.

$$\|\vec{u}\|_c^2 \;=\; \langle \vec{u} | \vec{u} \rangle_c \;=\; \frac{1}{2} \int_V (9\, u \cdot u + 9\, v \cdot v + w \cdot w)\, \mathrm{d}V\,, \tag{2.8}$$

Visualizations of trajectory (2.6) are of necessity projections onto two or three dimensions. A physically appealing choice [29] is to monitor the flow in terms of the symmetry-invariant and physical energy, dissipation and power input observables $(E(t), D(t), I(t))$. If two fluid states are clearly separated in such plot, they are also separated in the high-dimensional state space, but converse is not true; physically distinct states might have comparable energies, and such plots may obscure some of the

most relevant features of the flow. Furthermore, relations such as (2.5) depend on detailed type and geometry of a given problem [30, 31], and further physical observables beyond $(E(t), D(t), I(t))$ are difficult to construct. [7]

More straightforward are projections based on choices of several Fourier components (2.4) or other primitive basis elements as coordinate axes for projections of the flow. They are appropriate for small perturbations off laminar state, but such coordinate axes are (i) arbitrary and discretization-method dependent, and (ii) point in unphysical directions, far from turbulent states which in a highly nonlinear flows are characterized by many strongly coupled Fourier modes of comparable magnitude.

Recently, Gibson *et al.* [3] have shown that the dynamics of different regions of state space can be elucidated more profitably by a computationally straightforward choice of *physical* coordinates. One identifies several prominent states of the flow $\mathbf{u}_A$, $\mathbf{u}_B$, ..., such as equilibrium states and their eigenvectors, states in whose neighborhoods the turbulent flow spends most of the time, and from them constructs, by Gram-Schmidt or (anti)-symmetrizations, an orthonormal basis set $\{\mathbf{e}_1, \mathbf{e}_2, \cdots, \mathbf{e}_n\}$. The evolving fluid state $\mathbf{u}(t)$ is then projected onto this basis using the inner product (2.7),

$$a(t) = (a_1, a_2, \cdots, a_n, \cdots)(t)\,, \qquad a_n(t) = \langle \mathbf{u}(t) | \mathbf{e}_n \rangle\,. \tag{2.9}$$

This low-dimensional projection can be viewed in any of the $2D$ planes (a_m, a_n) or in $3D$ perspective views (a_ℓ, a_m, a_n), see figure **??**. The state-space portraits are dynamically intrinsic, since the projections are defined in terms of intrinsic solutions of the equations of motion, and representation independent, as the inner product (2.7) is independent of the numerical discretization. It is worth emphasizing that the method affords low-dimensional *visualization* without any low-dimensional *modeling* or dimension reduction; the dynamics are computed with fully-resolved direct numerical simulations. Although the use of particular relative equilibria to define low-dimensional projections may appear arbitrary, such a choice turns out to be very useful when the turbulent flow is chaperoned by a few invariant solutions and their unstable manifolds, as has been shown in other low Reynolds number settings [3]. Such visualizations are a prerequisite to uncovering the interrelations between (the infinite number of) invariant solutions, and constructing symbolic dynamics partitions of state space needed for a systematic exploration of turbulent dynamics, the key challenge that we address here for the case of turbulent pipe flows.

2.2.2 Charting the slice

[2012-06-06 Predrag] An excerpt from ref. [19] (click here for the full paper).

Let us summarize the voyage so far: We are charting a curved manifold, and it would be nice to use tools of differential geometry, but try it in 61,506 dimensions. The only feasible way to chart this space is to (1) quotient all continuous symmetries, and (2) tile it with flat $(61,506-N-1)$-dimensional tiles, or charts. We do it step by step, starting with a set of templates and using them to construct charts of each neighborhood, and

[7] Predrag: add here references to (2.5) derivations. Does Frisch [32] do it?

then building up an atlas of the *slice*, chart by chart, which captures all of the reduced dynamics of interest (but not all possible dynamics). Here are the steps along the way:

Template Pick a template $\hat{a}'$ such that G acts on it regularly with a group orbit of dimension N.

Slice hyperplane The $(d-N)$-dimensional hyperplane satisfying $\langle \hat{a}|t'_a\rangle = 0$, normal to group transformation directions at the template $\hat{a}'$.

Moving frame For any a, the slice condition $\langle \hat{a}|t'\rangle = 0$ on $a = g(\phi)\hat{a}$ determines the moving frame, i.e., the group action $g(\phi)$ that brings a into the slice hyperplane.

Chart border The set of points $\hat{a}^*$ on a slice hyperplane whose group orbits graze the hyperplane tangentially, such that $\langle \hat{a}^*|t'\rangle = \langle t(\hat{a}^*)|t'\rangle = 0$.

Flow invariant subspace If a subset or all of the group tangents of a chart border point $\hat{a}^*$ vanish, $t_a(\hat{a}^*) = 0$, its time trajectory remains within a flow-invariant subspace for all times.

Ridge A hyperplane of points $\hat{a}^* \in \mathcal{P}^{(21)}$ formed by the intersection of a pair of slice hyperplanes $\hat{\mathcal{M}}^{(1)}$ and $\hat{\mathcal{M}}^{(2)}$.

Chart The neighborhood of a template $\hat{a}'^{(j)}$, bounded by the chart border and the ridges to other linear neighborhoods, comprises a *chart* $\hat{\mathcal{M}}^{(j)} \subset \mathcal{M}/G$. The borders ensure that there is no more than one oriented group orbit traversal per chart; a group orbit either pierces one chart, or no charts at all.

Atlas A set of $(d-N)$-dimensional contiguous charts $\hat{\mathcal{M}}^{(1)}, \hat{\mathcal{M}}^{(2)}, \cdots$

Slice Let G act on a d-dimensional manifold $\mathcal{M}$, with group orbits of dimension N or less. A *slice* is a $(d-N)$ dimensional submanifold $\hat{\mathcal{M}}$ such that all group orbits that intersect $\hat{\mathcal{M}}$ do so transversally and only once.

In literature [33, 34, 35] 'slice' refers to any co-dimension N manifold that slices transversally. Here we define an atlas over a slice constructively but more narrowly, as a contiguous set of flat charts, with every group orbit accounted for by the atlas sliced only once, and belonging to a single chart. A slice is not global, it slices only the group orbits in an open neighborhood of the state space region of interest.

The physical task is to, for a given dynamical flow, pick a set of qualitatively distinct templates (for a turbulent pipe flow there might be one typical of 2-roll states, one for 4-roll states, and so on) which together provide a good atlas for the region of $\mathcal{M}/G$ explored by chaotic trajectories.

The rest is geometry of hyperplanes and has nothing to do with dynamics. Group orbits $\hat{\mathcal{M}}^{(j)}$, group tangents $t(\hat{a}'^{(j)})$, and the associated charts are purely group-theoretic concepts. The slice, chart border and ridge conditions are all linear conditions which depend on the ray defined by the template $\hat{a}'$, not its magnitude. Checking whether the chart border is on the far side of the ridge between two slice hyperplanes is a linear computation; for a symmetry-reduced trajectory moving in $\hat{\mathcal{M}}^{(1)}$ chart one only has to keep checking the sign of

$$\langle \hat{a}(t)|t'^{(2)}\rangle \,. \tag{2.10}$$

Once the sign changes, the ridge has been crossed, and from then on the trajectory should be reduced to the $\hat{\mathcal{M}}^{(2)}$ chart. For three or more charts you will have to align the ridge of the current chart with a previously-used chart. You'll cross that ridge when you come to it (a hint: the manifold is curved, so there will be a finite jump in phase).

It is worthwhile to note that the only object that enters the slice hyperplane, border and ridge conditions is the ray defined by the unit vector $\hat{t}' = t'/\|t'\|$. This gives much freedom in picking templates.

With the atlas in hand, the dynamics is fully charted: as explained in refs. [14, 21], Poincaré return maps then yield all admissible relative periodic orbits.

Three concluding remarks on what slices *are not*:

(1) Symmetry reduction is not a dimensional-reduction scheme, a projection onto fewer coordinates, or flow modeling by fewer degrees of freedom: It is a local change of coordinates with one (or N) coordinate(s) pointing along the continuous symmetry directions. No information is lost by symmetry 'reduction', one can go freely between solutions in the full and reduced state spaces by integrating the associated reconstruction equations.

(2) If the flow is also invariant under discrete symmetries, these should be reduced by methods described in ChaosBook.org.

(3) An atlas is *not needed* for Newton determination of a single invariant solution, or a study of its bifurcations. [36] Any local section and slice plus time and shift constraints does the job. 60,000 relative periodic orbits can be computed this way. [31] Once we have more than one invariant solution, the question is: How is this totality of solutions interrelated? and for that a good atlas is a necessity.

Chapter 3

Blog

I am usually as happy as possible in any situation.
— Joe

3.1 Daily blog, point by point

now in CB

2011-05-27 Predrag, weather report from Snowbird DS11 Learned from Pierrehumbert that the baroclinic models are to weathermen what "harmonic oscillator" is to quantum mechanics. It has a continuous East-West translational symmetry, i.e., in a periodic box it needs to be sliced (the SO(2) of periodic box quotiented out).

Tried to proselytize Christian Wolfe [37], Scripts, make him slice the baroclinic instability, and, perchance, if I get him there, recycle it, former Gibson style. Pierrehumbert says that this would be persuasive to weather people, convince them to go looking for exact unstable invariant solutions. After one hour Wolfe said he was converted.

Tried ditto with Pierrehumbert and Silber postdoc Yi-Ping Ma (Knobloch trained, has worked with Spiegel at Woods Hole GFD). He does not know any geophysical fluid dynamics yet, so I'm sceptical that he will do anything.

2011-05-27 Annalisa Bracco If you ever need a code that produce baroclinic instability, I have plenty. Worked with the Joe Pedlosky, the expert on Baroclinic Instability, as a postdoc. I also have an easy atmospheric model (global, on a sphere etc) that reproduces very well baroclinic instability as per observations and can be run as aqua-planet to simplify things.

2011-05-27 Predrag We could make Joe Pedlosky happy? Let's do it before August, in time for Woods Hole. The first step is to slice your simulations for a minimal periodic cell of interest (narrow but turbulent). The second step might be either to determine "physical dimension" using Wolfe-Samelson [37] Lyapunov

vectors (that is just simulation) or find some traveling waves (that is Krylov-Arnoldi nontrivial work, but for low-dimensional discretizations might be doable by Newton).

2011-10-15 Annalisa Shown Predrag some simulations. Each layer is computed in terms of vorticity equations as a 2-dimensional fluid. The lower layer has higher fluid density, and they are coupled across their interface by difference of vorticity. In our simulation this is about factor two; it is related to the Rösby deformation radius L_R. The spanwise y width is $L_R/2\pi = 1/2$. Unless the width is larger than L_R, no instability. The stream-wise aspect ration is about 8. They tend to the barotropic solution (vortices rotating the same way on top and bottom).

Discussion of solutions:

1) is linear: dropped the nonlinear term i.e. the Jacobian of the vorticity and the stream function. Instability is seeded by a small random field of prescribed power spectrum, but the resulting instability is a localized wave (about 3 rolls) with streamwise/spanwise ratio of about 1/2 set L_R. That sets the scale of the instability off the laminar solution. Initial noise does not matter, as the instability grows very fast. The two layer vorticities are opposite.
2) is fully nonlinear, all other parameters the same.

2011-10-18 Annalisa Figure 3.1 (a) The usual domain $L = 8$, 2 layers. Note that as for initial conditions, the overall the flow is more energetic.

Figure 3.1 (b) The reduced domain $L = 4$, 2 layers. Correct initial conditions, starting from a linear solution. The energy is not yet fully equilibrated. One problem I can see is that the periodic boundary conditions may prevent perfect equilibration. The longer cell Figure 3.1 (a) behaves pretty much the same way, but overall the circulation is a bit stronger.

2011-10-19 Annalisa There is a barotropization issue, likely due to the periodic boundaries. My guess is that we'll not need a very long simulation and we can live with a non perfectly stationary state, essentially the eddies that form in the equilibrated solution prefer to be barotropic -same sign top and bottom layer- because they are more stable and in the absence of viscosity they are an exact solution of Navier-Stokes, and the simulation goes into a state that resembles the long-term state for 2-d turbulence. If we could work only over times $\sim$40-70 we should be all set.

For now the time is just in code units, I'll convert it in something meaningful once we decide on which run to use, etc..

2011-10-20 Predrag Bit worried if we are in transient turbulence, on the way to a barotropic state, but might work out...

2011-10-20 Annalisa One way to reduce the problem may be to stick to the 'longer' domain. Another is to introduce a sponge region on one side. It will not solve

the problem completely: eddies are just more stable if barotropic and they tend to become so while equilibrating a baroclinic solution, but it may delay it.

2011-10-20 Predrag It's OK that whole thing decays to barotropic, as long as we can find unstable equilibrium solutions. Next (big) step. The short step is to start looking at the dynamics of a short domain in the state space, as explained in ChaosBook.org/tutorials, click on 'state space' in the menu on the left.

2011-10-20 Annalisa I may be able to stabilize it in a weakly nonlinear regime without vortices but still something going on. I checked Wolfe PhD thesis and it's all done in a very weakly nonlinear regime, so waves (just not perfectly regular).

2011-10-20 Edward A. Spiegel Baroclinic instability is a buoyancy driven instability in which horizontal gradients and rotation play complicating parts. Basically, because of effect of rotation, the displacement of a fluid parcel that unleashes the instability is not vertical as in R-B convection. Or, if you prefer, in the presence of rotation, your notion of what is vertical is changed.

Pedlosky has written GFD lectures that do a pretty good job of explaining the stuff. If you are face to face with the right person, such as Joe, it is no problem. I think you should read a bit first and then talk to a person. Anyway, it is time for you to test the waters of GFD books. For agreeable starts try Rick Salmon [7] or James Holton [6].

Then talk to someone.

I once supervised a summer GFD project on baroclinic instability, A. E. Hasha (2005) report *A Search for Baroclinic Structures* and I think it made a nice self-contained package. You may not want to start with that heavy a story. I have some easier stuff but I have no idea where you put it so I can say only that you should look for the term "Eady problem."

2011-10-20 Predrag 2 EAS Funny thing is I was reading Hasha when your email arrived. Nice report. I can be more specific:

When I look at Annalisa's 2-layer simulations (driven at top by a constant velocity field, streamwise length = 8 channel widths, Rossby number = 2) it looks to me that baroclinic vortices get converted onto barotropic ones, and there is nothing that would sustain generation of new baroclinic vortices (opposite vorticity in the two layers), so there is no sustained turbulence, it looks only transient. Or am I missing something?

2011-10-21 EAS This sounds like a case for cyclic behavior. If you keep running Annalisa's case, I presume the barotropic vortices will run down and the baroclinic instability will come back. That is, when the barotropic vortices decay, you go back to the baroclinically unstable situation and it all starts over. Why it might do this instead of staying in a mildly unstable, statistically steady case all the time is a bit of a mystery. (Are you sure that it does not?) There are other examples where systems go cyclic in this way instead of maintaining a quasi-steady mean state but I have not found the clue to predicting which case one will get. For example, why do things go all barotropic in your case?

2011-10-21 Annalisa OK, but it'll take a LONG time, because the dissipation time of relatively large, single eddies is pretty small. This is one of those situations where the model domain plays such a role that the 'real' application is close to null.

2011-10-22 Predrag 2 Annalisa I'm working on writing up the physical ways of projecting turbulent flows onto handful of state space coordinates. The derivation of the first set, $(E(t), D(t), I(t))$ and generalizations is illustrated by a simpler case, the Kuramoto-Sivashinsky equation, in sect. **??**. I'll try to get to the Navier-Stokes case and the much better Gibson et al. coordinates, but it is taking time...

2011-10-24 Annalisa Still not convinced about the flow field per se. Figure 3.2 and Figure 3.3 are plots of the vorticity in the top layer at 3 different times during which the energy is $\approx$ stable (at least the kinetic part, but being dominant also the total is OK). The problem is that the structures I see are always the same, they are just moving a bit. And this is going to be the case with this channel once is equilibrated.

BTW, Lo Specchio is theoretically right, but practically wrong. Barotropic vortices can take a long time to dissipate. By that time, everything else dissipated as well (i.e., any residual perturbation of the flow field) and there is nothing on which the baroclinic instability will be able to feed upon: if you start with zero perturbation field in the Phillips model, you'll still end up with zero perturbation everywhere.

2011-10-20 Predrag I understand - they are sort of frozen in. In spatiotemporal chaos it is one of the possible phases of an extended system, but for weathermen, this is no fun at all. There must be something to baroclinic instability that I am missing - it cannot be that it is just a complicated transient? In that case we might have to drive it by noisy surface winds, but that will be harder...

2011-10-24 Annalisa My take on baroclinic instability: wonderful linear theory. Practically useful only to figure out where you form eddies. I can still try to reduce further the dimension of the domain and see what happens in that case...

2011-10-20 Predrag Something quite different but of interest to me; the reason you always see spirals in these N-layer models is that locally $2D$ fluid mechanics is Euclidean-invariant? In a full $3D$ simulation these vortices would still be there because of horizontal layers of fluid of equal density?

2011-10-24 Annalisa Personal take on the spirals... It looks that is the best way for the eddies to barotropize. There must be some energy conversion mechanism that favors them.

2011-10-24 Annalisa The physics of 2d turbulence is .. 2d turbulence. It creates vortices. More relevant for the ocean than the atmosphere, but baroclinic instability creates vortices as well.

2011-10-25 Annalisa, Predrag, Joe Pedlosky (conference call, Joe office 508-289-2534, home 508-548-2069; Annalisa cell 404-323-7722, office 404-323-7722, home 404-724-0975; Predrag 404-IT-STINX everywhere)

Annalisa I'm running 2-layer Phillips model, driven by fixed velocity at the surface, bottom layer is at rest. Use $\beta = 0$; tried with $\beta \neq 0$, but it makes no difference. In linear solution, instability kicks in, goes unstable linearly *very* fast. In nonlinear regime it does not get into equilibrated state, nonlinear term wants to generate spirals which then drive the flow into barotropic state.

Joe What maintains the flow?

Annalisa Specifying initial zonal velocity - maintain constant current on the top layer, always there. Friction is Newtonian viscosity in both layers. Deformation radius (PC: Rossby number?) is such that the channel is twice that. I tried with 4 times the radius, nothing changes.

Joe Even though is baroclinicity is maintained by constant surface drive? Flat 2-layer model requires $F =$(wavenumber)$^2/2\pi \approx 5$, a fairly large number. In your setup baroclinic instability is maybe not driving. In our simulations we get baroclinic production everywhere in the bulk for $F \approx 4$.

What if viscosity only in the bottom layer?

Annalisa In literature I never saw equilibrated 2-layer Phillips.

Joe A man called P, but not me, from Texas A& M had a number of simulations, looking for equilibrated state. The references are Panetta [38, 39] and Pedlosky [40]

Predrag: alert me if we should read any of the related refs. [41, 42, 43, 44], or refs. [45, 46, 47, 48, 49, 50, 51, 24, 52, 53, 54, 55].

2011-10-26 Annalisa I read the papers Joe' suggested. Two have no vortices (the 1d Panetta [38] and the one by Joe [40]). The Panetta [39] may be relevant but very limited resolution (so vortices may not form in that case as well. Hard to say from just streamfunction plots). Still Panetta does reach an equilibrium state. Set-up pretty similar (except for periodic conditions). I wrote exactly that code, but in 2000, and I don't have a copy (lost somewhere in Torino). Not sure when I can re-write it from scratch if necessary (need really to write a paper first).

Alert Joe that the figures are at the end of this text (I can also make plots of the energy in time). The equations need some correction.

2011-10-26 Joe Thanks for the creature from the Blog Lagoon?. I have really one very simple question that I could not find in the write-up.

What is the width you use to scale the horizontal lengths? Or, more specifically, what is the ratio of the width of the channel to the deformation radius? I am trying to see what the value of the parameter

$$F = (f^2 L^2)/g' H$$

is in your calculations where H is the depth of each layer and L is the channel width.

2011-10-26 Annalisa I tried with different sizes, but always in what should be an unstable regime according to the Phillips criteria and our old calculations with the same code (and it always is unstable in the linear case). I modified all the numbers twice since the simulation shown in the notes, so I'm not 100% sure (anyway, that run is useless), but I usually set $F = 1$ 'model unit' and the width of the channel has been varied between π and 2π (4π as for yesterday and still nothing). Starting to think I may have made a mistake somewhere while removing the topography term from the old code and somehow I'm not getting the upper current in the non-linear calculations, because it makes no sense.

2011-10-28 Annalisa Fixed the bug in the top layer driving term, see figure 3.5. The kinetic energy figure 3.6 is still growing, but the potential is stable. I'll play with the dissipation. There is still a tendency for the eddies to barotropize (no reason that should change), so not sure if the kinetic energy will ever get perfectly stable (unless I dissipate a lot).

2011-10-28 Predrag Talked to John Gibson, Skype johnfgibson. He thinks it would be easiest to append his Newton-Krylov-Arnoldi solvers to your code - you guys can talk about it.

2011-10-28 Annalisa You seem to have an automatic forward to some gmail account with a limited size allowed If you wish to look at the second one, let me know and I'll send it separately.

2011-10-28 Predrag You are using Mac at work, or Linux, or?

2011-11-09 Annalisa Figure 3.8 is a run with much lower (10 times lower) large scale dissipation. Not perfectly equilibrated though, see figure 3.7.

I'll remove the dissipation at large scale in the top layer, convert the operator into Ekman and see if I can get a stationary state if you think is still worth it.

2011-11-09 Predrag The plots are pretty. I think removing the dissipation at large scale from the top layer, and converting the operator into Ekman would be more physical. If you can get a stationary state we could at least use it for motivational purposes for the AGU meeting.

I'm worried about plotting potential vs kinetic energy - their sum might be approximately conserved, masking turbulent dynamics. It would be better if you can plot the rates such as power in, dissipation out in (2.5).

2011-11-23 Annalisa In figure 3.9 and figure 3.10,
E_K =kinetic comp
E_P =potential
E =total (sum of the two)
$E_{baroclinic}$ is only the baroclinic contribution to the kinetic term ($E_K = E_{barotropic} + E_{baroclinic}$) D includes large scale contribution from Ekman term and small scale (newtonian viscosity) from both layers. It is dominated by the large scale though The nomenclature for the derivatives is obvious.

I don't see anything that compares too well to the plots you showed me...

2011-12-06 Predrag In my struggle to avoid dealing with preparing the AGU talk, I was trying to figure out how to convert Woods Hole prehistoric FLIC formatted `vort.fli` into flash, or anything. Fli2Gif might work in Linux. Then my friend David clipped it and converted it to 6MB

`dasbuch/WWW/tutorials/Movies/baroclinVort.flv 1020×900`,

just like that. Turns out AGU does not allow internet access from the lecture PCs, so I had to convert my ChaosBook.org/tutorials slides into PDF. Thankfully, Acrobat allows inclusion of Flash movies - the result is

`siminos/talks/AGU11talk.pdf`.

It is 38MB, so I have not added it to svn; ask me if you want a copy.

2011-12-12 Francesco Fedele I came across the arXiv:1112.0151 paper on the linear stability of pipe flows for almost periodic perturbations (with irrational frequency ratios) there is instability at $\mathrm{Re} \sim 140$..

2012-01-13 Predrag We should organize this seminar: Francesco Fedele
Assistant Professor
School of Civil & Environmental Engineering
School of Electrical & Computer Engineering

Title: *From Hamiltonian equations for the ocean dynamics to traveling waves in Axisymmetric Navier-Stokes Equations*

Abstract: In this talk I will present an overview of recent results on the Hamiltonian formulation of envelope equations for the ocean wave dynamics and experiments for stereo video measurements of oceanic waves off the Venice coast in Italy. In particular, wave dispersion and energy cascades observed experimentally confirm that ocean waves can be thought as a state of weak wave turbulence, i.e. a state of weakly nonlinear interactions of dispersive elementary waves, the analogue of vortices in strong Navier-Stokes turbulence. In this regard, I will also discuss a model reduction of the axisymmetric Navier-Stokes equations for pipe flows and the existence of traveling waves. In particular, small perturbations of the laminar flow with amplitude $\epsilon \approx O(Re^{-2.5})$ obey a coupled system of nonlinear Korteweg-de Vries type equations, which support inviscid soliton-type solutions and periodic waves in the form of toroidal vortex tubes.

2012-02-07 Predrag Added Sebastian Ortega Arango <sortega@gatech.edu> project to this blog; enabled svn access, updates (sortega baroclinic). See chapter 4.

2012-02-09 Predrag Should read *Hamiltonian description and traveling waves of the spatial Dysthe equations*
by Francesco Fedele and Denys Dutykh, arXiv:1110.3605.

2012-04-17 Denys Dutykh to Predrag (HREFhttp://www.linkedin.com/in/dutykh/web site, Francesco Fedele's collaborator) Before attacking the full Euler with free surface, we would like to play with toy-models in our field like KdV, for example, to start to apprehend this technology of periodic orbits.

I will take care of numerics. It is my passion.

2012-02-17 Predrag Francesco Fedele want us to read Boccotti [56], in particular ref. [57] (I have stored it in CNS Zotero account). Francesco says: " a paper on the recurrence of large waves in the ocean ... real data from experiments in the Mediterranean sea in South Italy .. the sea is very special there :) .. really .. perfect wind waves all the time ... experimental site suitable to test theories, etc..

I have another space-time set of data (wave surface in space and time $\eta(x, y, t)$ over an area of $100^2 m^2$ and duration 1 hour) collected near Venice and I would like to check recurrence using Poincaré-based approaches. That would be a good start. "

2012-06-05 Predrag Should read *Effect of differential diffusion and extrapolated Ekman dissipation on flux constraints on the two-layer quasi-geostrophic model* by Eleftherios Gkioulekas, arXiv:1206.0315? He says: " We continue our investigation of an inequality constraining the energy and potential enstrophy flux spectra in the two-layer quasi-geostrophic model. Its physical significance is that it can diagnose whether any given model that allows coexisting downscale cascades of energy and potential enstrophy can reproduce the Naström-Gage spectrum, in terms of the total energy spectrum. This inequality holds unconditionally for two-dimensional turbulence, however it is far from obvious that it generalizes to multi-layer quasi-geostrophic models. In previous work we considered the case of a two-layer quasi-geostrophic model in which the dissipation terms for each layer are dependent only on the streamfunction field of the corresponding layer. We now generalize this configuration as follows: First, following a 1980 paper by Salmon, we use an extrapolated Ekman term at the bottom layer which uses the streamfunction field of both layers to approximate the streamfunction field at the surface boundary layer. Second, for reasons explained in detail in the paper itself, we use small-scale dissipation terms with different hyperviscosity coefficients. Sufficient conditions for satisfying the flux inequality are given under this more general dissipation configuration, and we discuss the potential role of extrapolated Ekman dissipation and differential small-scale dissipation in violating the flux inequality. "

2012-06-05 Annalisa I just turned down the invitation from JFM to review that manuscript because I'm leaving for the cruise in the gulf tomorrow... not sure is relevant (and pleased I turned down the review, now that I see the full manuscript...)

2014-07-09 Predrag Added the abstract for my 2014 Woods Hole talk:
`siminos/baroclinic/GFD14.tex`, on Aug 4. The course is all about baroclinic stuff - isn't this time to make a big push?

2014-07-09 Predrag Gave my 2014 Woods Hole talk:
`siminos/talks/WoodsHole14/` Mostly a programmatic talk. It is my only talk that defines baroclinic instability.

It also keeps symmetry reduction to almost no formulas.

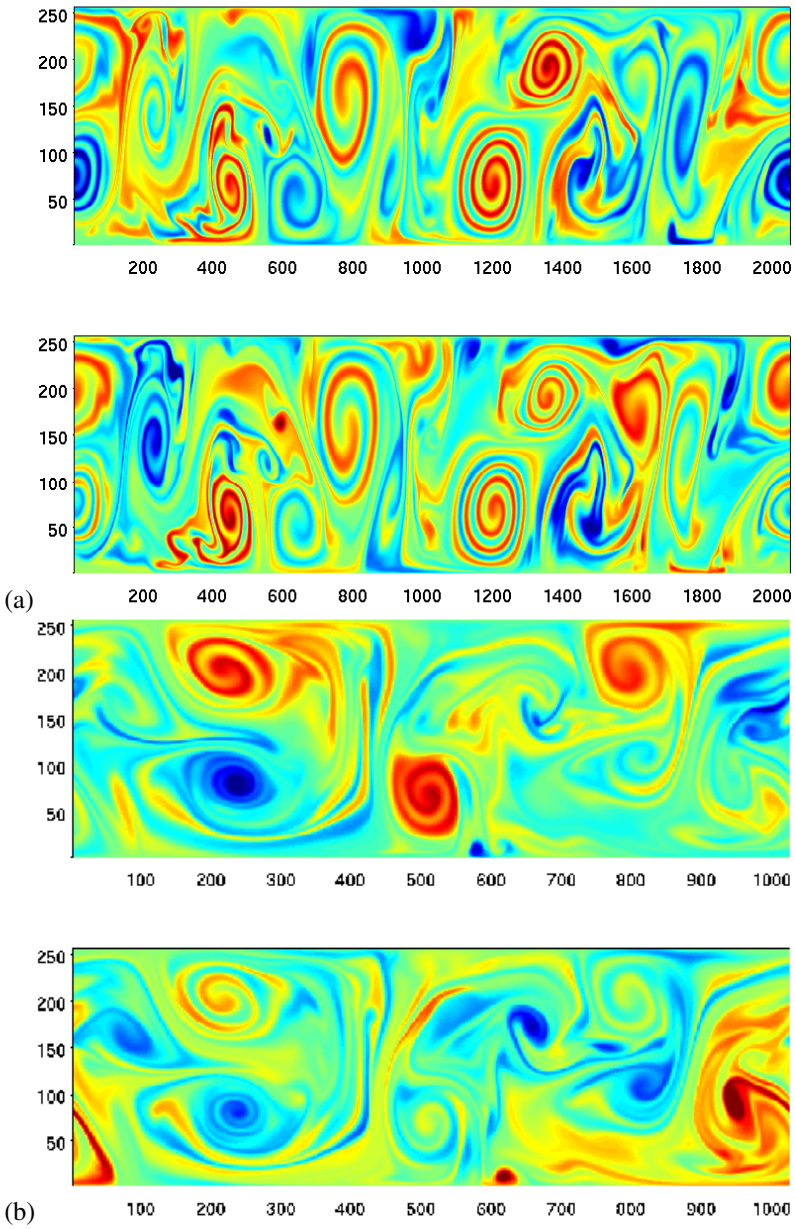

Figure 3.1: 2 layers: top, bottom. (a) The usual domain $L = 8$. (b) The reduced domain $L = 4$, initial conditions starting from a linear solution. The energy is not yet fully equilibrated. The longer cell (a) behaves pretty much the same way, but overall the circulation is a bit stronger.

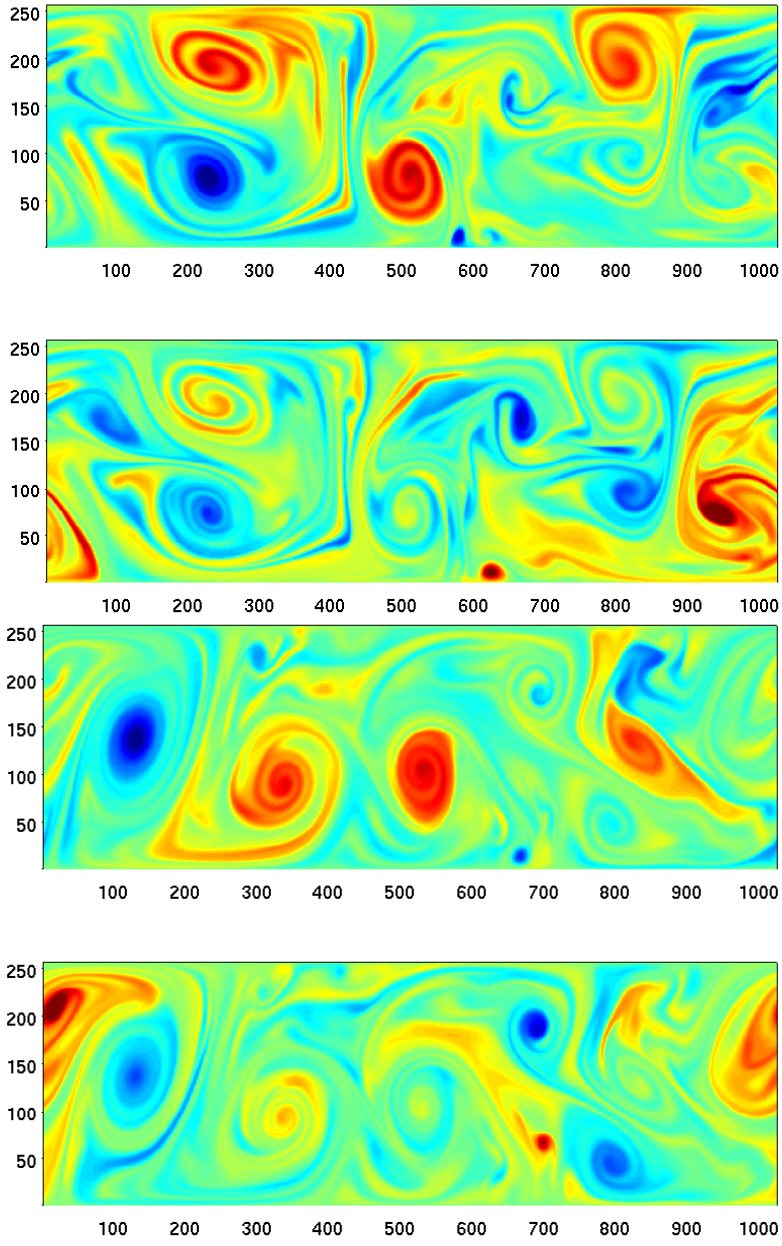

Figure 3.2: A plot of the vorticity in the top/bottom layers at times 50 and 70.

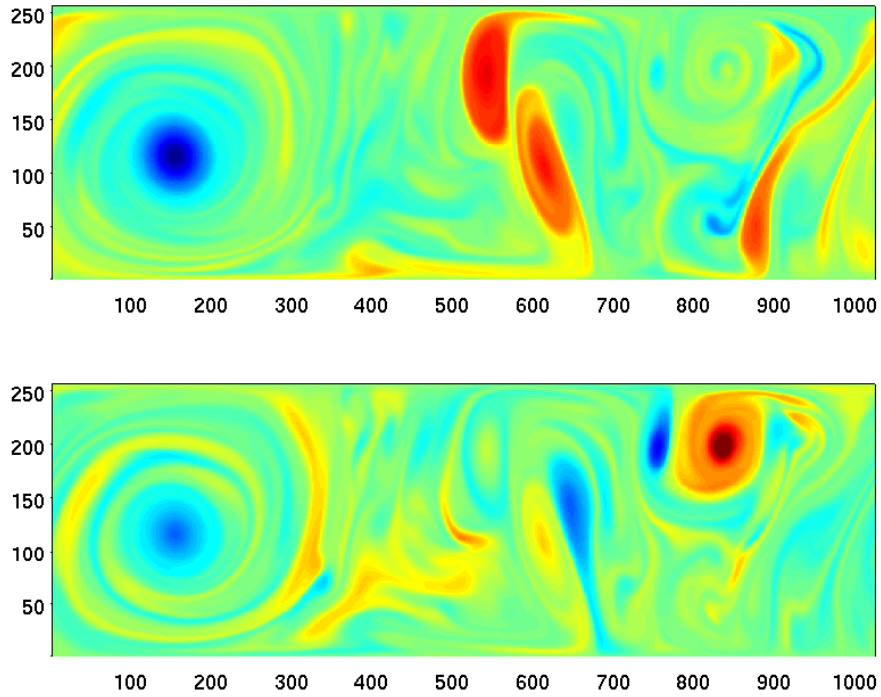

Figure 3.3: A plot of the vorticity in the top/bottom layers at time 100.

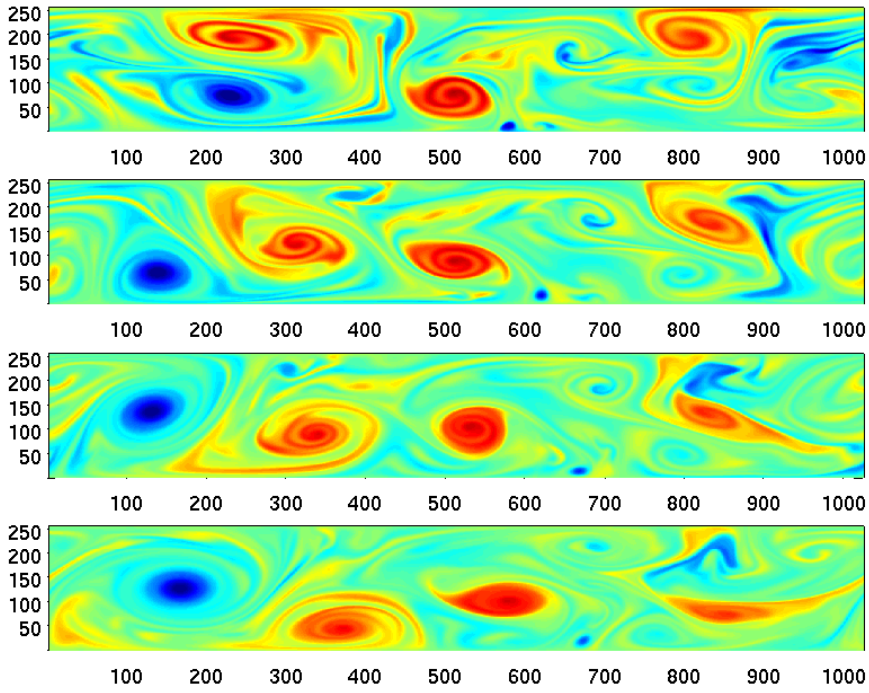

Figure 3.4: A plot of the vorticity in the top layer at 4 different times during which the energy is $\approx$ stable. The structures remain the same, they are just moving a bit.

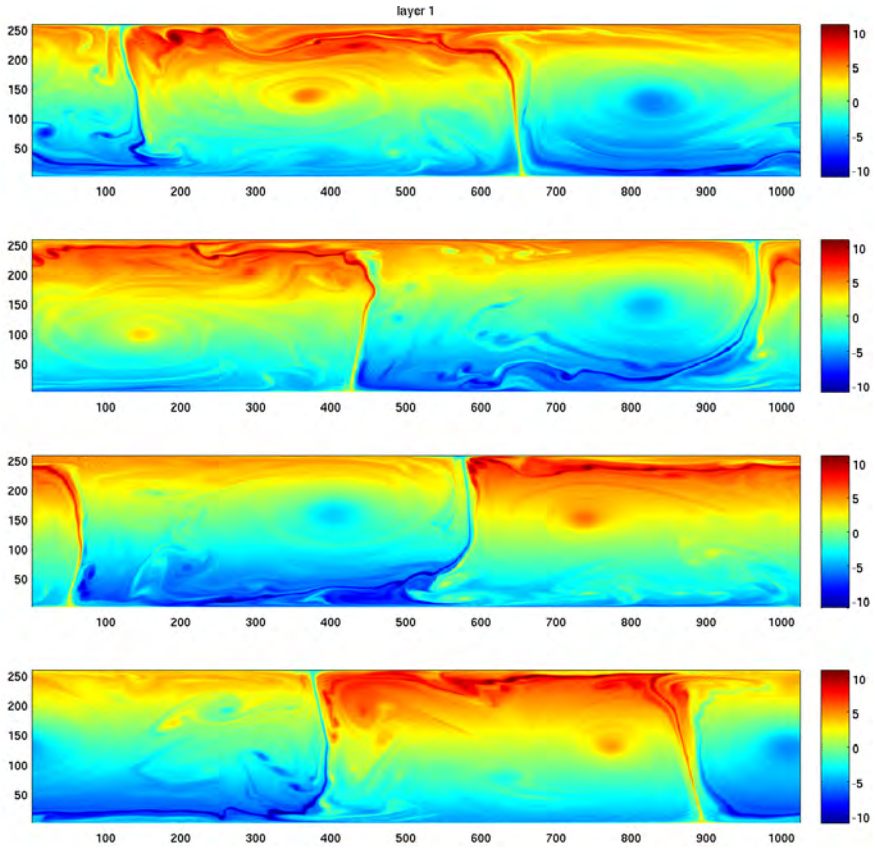

Figure 3.5: The top-layer fixing term now corrected (all previous figures are wrong). A plot of the vorticity in the top layer at 4 different times, but energy is still increasing, see figure 3.6.

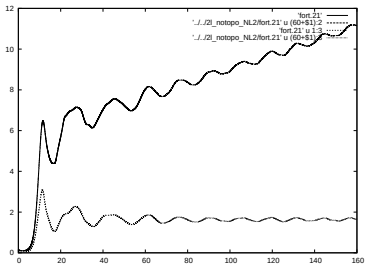

Figure 3.6: The kinetic energy for the evolution of figure 3.5. To Predrag the top curve looks monotonically increasing (energy cannot do that, and the pictures of flow do not look like they are speeding up) and he has no idea what the bottom curve is.

(*a*) (*b*)

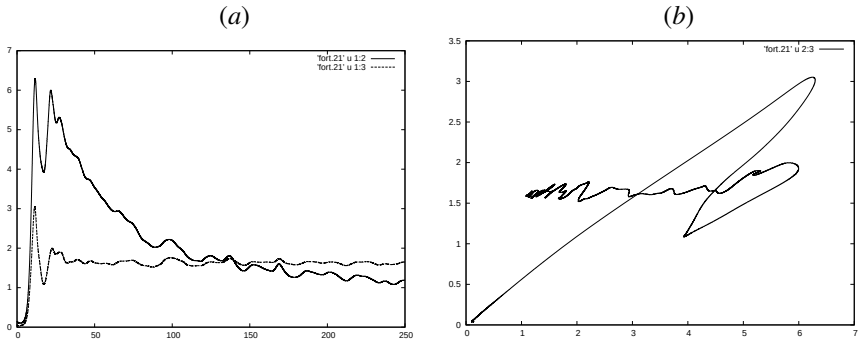

Figure 3.7: The kinetic and potential *vs* kinetic energy plots for the evolution of figure 3.8.

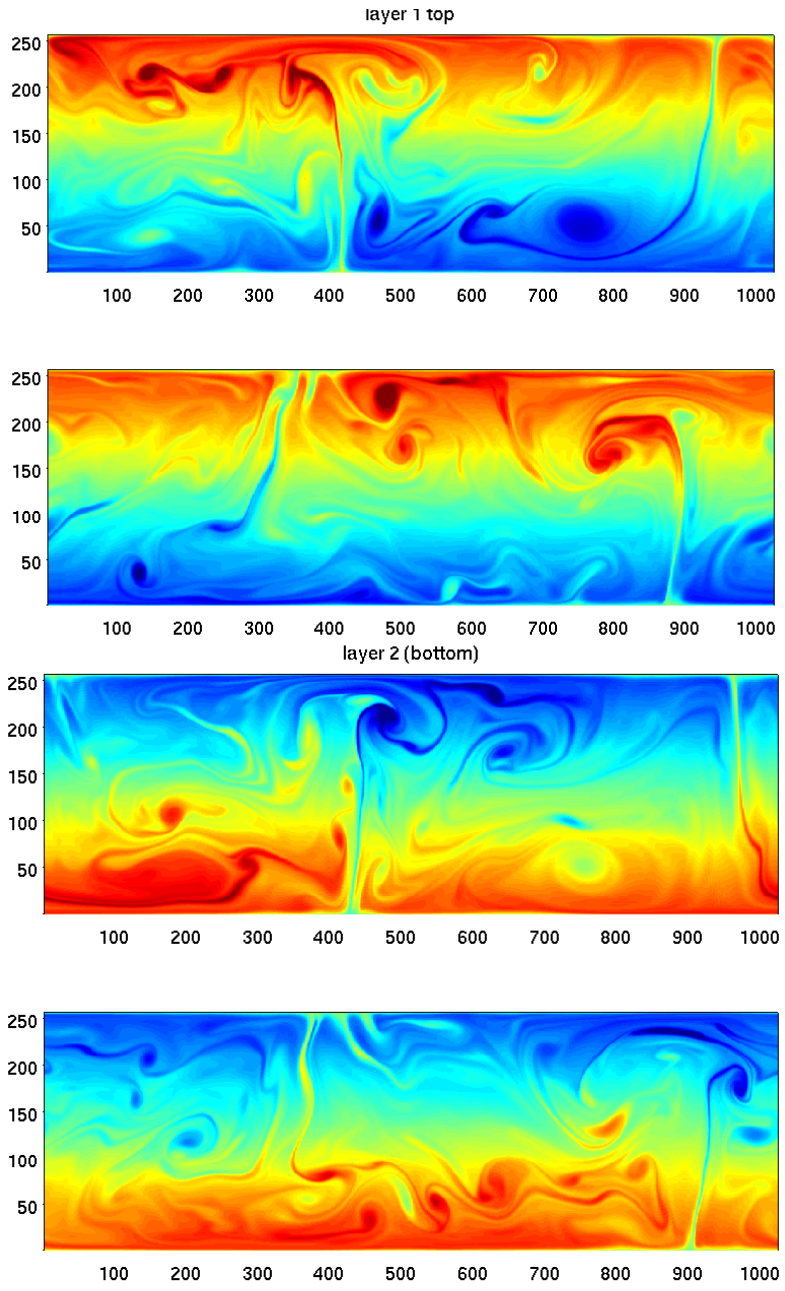

Figure 3.8: A plot of the vorticity in the top/bottom layers at times ?0 and ?0.

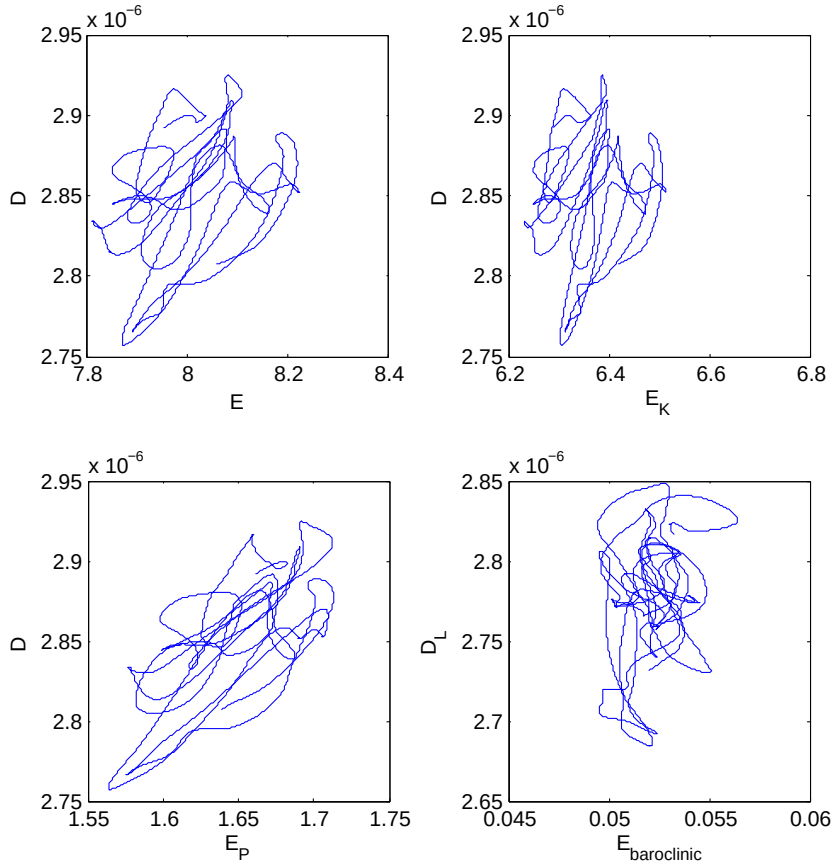

Figure 3.9: Energy plots. See also figure 3.10.

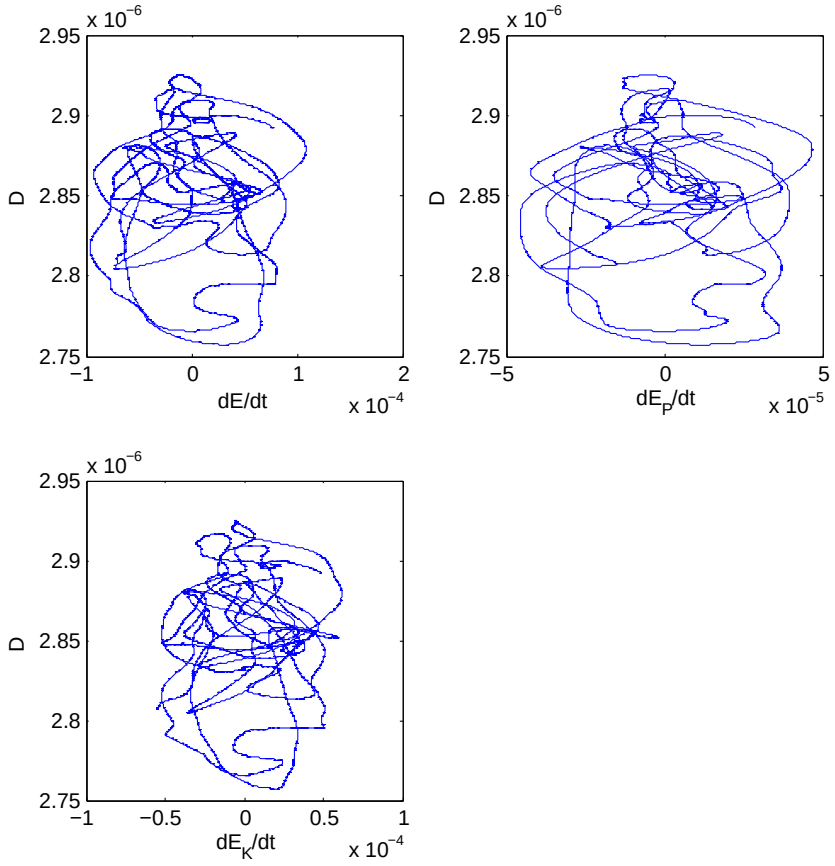

Figure 3.10: Energy rates plots. See also figure 3.9.

Chapter 4

Convectively coupled waves

4.1 Introduction

2012-02-08 Predrag Please write an introduction to the "Convectively coupled waves" suitable to inclusion into your thesis: what they are, and why should one care. Add relevant references to this repository's siminos/bibtex/siminos.bib (no separate bibliographies, it makes updating them a pain).

4.2 Sebastian's blog

This is Sebastian Ortega Arango's blog for PHYS 7224, spring 2012 *Nonlinear dynamics: Chaos, and what to do about it?* course project

2012-02-07 Predrag Added Sebastian Ortega Arango <sortega@gatech.edu> project to this blog; enabled svn access, updates (sortega baroclinic). First task: please study chapter 1, and improve it in any way you see fit, edit, add better references etc.

2012-02-07 Sebastian I think I would be able to relate the project with my line of research. I am interested in **Convectively Coupled Waves**. I read that people at NYU has worked the mathematics in this types of phenomena, and it appears that interesting nonlinearities arise from it. Baroclinic instability seems to bee an important driver.

2012-02-08 Predrag I would like the project to focus on a geophysically important model that exhibits $SO(2)$ invariance, hence propose to investigate the baroclinic instability first, then apply that to your thesis research on Convectively Coupled Waves. Advantage of starting with the baroclinic instability is that you can hit the ground running, as Annalisa has simulation code ready to use.

2011-10-15 Annalisa Define and explain the Rossby radius for the atmosphere in sect. 4.1. Mark here [ ] when done.

2012-03-27 Sebastian I am going to follow your advice and star working with baroclinic stability first. I have written a draft of the introduction, the idea is that it outlines the work to be done, and is subject to changes. I think it is a good outline to introduce baroclinic instability, and to introduce the model used in the simulations. However, it still not clear to me how to include the nonlinear analysis. I will continue reading about the Kuramoto-Sivashinsky equation and the plane Couette flow for this. I will try to write sect. 1.1 today.

2012-03-27 Predrag I'm glad you are getting started - go for it.

2012-03-27 Sebastian Also, I find a thesis that might be interesting to read Veen's thesis, Chapter 2.

2012-03-27 Predrag I have not read Lennart's thesis, but he does good work. Blog here what you find of interest as you read it.

2012-04-04 Sebastian Finished first and second section. I am uploading to show what I have done so far, but it is just a quick draft as far as redaction goes. I still have to read it again and correct it. Some times I write in this way, first I get all the ideas in paper and then iterate until I have a coherent document. Probably not the best way out there.

In short, the point that I am trying to get trough, is that there is a base flow given by geostrophy and the hydrostatic relation which might be stable depending on the slope of the isopycnals. Then I introduce the model Professor Annalisa used for her simulations (I believe is the one described by Philips in 1951).

I think it is important for me to get focus on the nonlinear aspects of the problem. So I will try to finish all the way to sect. 1.5 by this week (but not sure if I will have the time).

I was also wondering what should I do for the nonlinear section. But I guess I should first order my ideas and learn how to think of baroclinic instability in terms of dynamical systems. So far I think of it from the point of view of bifurcations (please correct me if wrong), where I have a equilibrium point in the dynamical system which becomes unstable (or disappears??) after some parameter increases (this is what I believe the linear theory does). But I am not sure what happens once the flow is unstable, my guess is that there would be some kind of strange attractor out there in the n-dimensional space. But I guess visualization of this would be quite hard, unless a low order spectral representation is used. It would be very interesting to hear your vision of the instability; so please let me know if there is a paper I can read for this, or what you think is happening.

Also, let me know of any changes that you think might be convenient.

2012-04-05 Sebastian A quote from Rick Salmon book (might be good for Chaos book). After proving Ertel's Theorem: "Of course, we can prove all these results directly from (1.1) by pedestrian mathematical manipulations, but that only makes it harder to appreciate their physical significance" **[2012-04-05] Predrag** added to the ChaosBook trove of reserve quotes, thanks!

2012-04-05 Sebastian Done with sect. 1.5 *Stability theory* text. However, some calculations are needed for the specific case (those for ω and U_c). But they might be in the literature somewhere; however there should be easy to do (or reduce easily from the ones given by Hasha [12] and/or Vallis [9]).

2012-04-23 Sebastian I have been trying to figure out how to find the fixed points and periodic orbits for my project. However, I am not really sure how to implement Viswanath GMRES algorithm to Annalisa's code (maybe a simpler one is ok, as Viswanath also look for relative periodic orbits). I think I have to write a searching algorithm based on the method, so I have been spending time trying to understand the solution method, although I have not fully understood it yet. I also found Halcrow theses in the web, this might help me figure out how to do it.

I think I will start writing down everything I have read, and what I think it might be found for the model. And then try to do code the searching algorithm. Let me know if you have any pointers for this, or if I should do something differently.

2012-04-23 Predrag I think implementing Viswanath GMRES algorithm to Annalisa's code is a semester project. It might be easier to implement her code as a module in channelflow.org, but that too is months of work. It is certainly worth doing, but you cannot do it in a week. I am happy if in your project right now you run her code, see some interesting structures, and maybe manage to find a close recurrence in the data.

Read the end of siminos/blog/blog.tex, chapter *Fluids* about this.

2012-04-23 Sebastian By the way, is there class tomorrow?

2012-04-23 Predrag Yes, this is the last week. If people want to, they can self organize to present their projects the coming week, but I'm not supposed to meddle, as it is exam week.

2012-04-23 Sebastian I guess I got a little exited about the papers I read; very interesting. I will try then to limit the search to recurrent motions. But will write about what can be done in the future. I have ran Annalisa's code already, so I will try to search this by looking at dissipation and energy plots as done in Viswanath to find an initial guess for periodic orbits. But my guess is that it would be very qualitative.

I was wondering what you think the implications of periodic orbit theory are for climate and weather. I have the feeling that it must be very important. But would like to hear what you think about it. I want to study predictability for my Phd work, focusing on the tropics intraseasonal variations (MJO and such); exploring this kind of approaches seem as something important to me. Let me know when you have time to discus this and I will go by your office.

2012-04-24 Sebastian Forgot to upload the blog yesterday. I am uploading it along with some advances in the nonlinear section (sect. 1.6 not yet complete). Just the ideas of some important papers I have found; and what I intend in doing for Chaos project. Currently I am running Annalisa's code for a longer period,

5 times more than before. And playing with the visualization of energies and dissipation to see if I can find close recurrences. I was also thinking in changing the parameters of the simulation. But I think I will try to find them first in the simulation as it is, and then change them if necessary. Any suggestions or recommendations are welcome.

2012-04-25 Predrag Here is my concrete proposal for what you can do now, for the course project. What you have written is good. What would really help us (Annalisa, me, you) is if you read the Chaos Gang paper (click here), and implement the sliced version of Annalisa's simulations. You do not need any invariant solutions to do this, use as a template a typical turbulent state in the simulation.

The key physical step is choice of norm, read commentary after Eq. (1). Slicing means that given the norm and the template, you replace ODE integrator velocity fields by the ones in slice, Eq. (8): these videos should be much calmer than the original simulation, as drifts have been quotiented out. That is already enough to complete the term project.

Next keep track of phase velocity Eq (9). If that diverges it means you are falling of the edge of your template's chart: you should use a multiple chart atlas. If you get a few charts, ridges, and reduced flow that encounters no singularities, we already have a publication.

Finding invariant solutions is essential, and cannot be done without symmetry reduction, but it not necessary to illustrate symmetry reduction.

2012-04-25 Sebastian Will try to do so. But the representation as in (1.38) is still not clear to me from the code. The vorticity and the stream functions both change in time and one depends on the other ($\xi = \nabla^2\phi$). However, the equations are solved for the vorticity with a Adams-Bashforth integration. So maybe I can just forget about the stream functions and think of the system as $d\widehat{\xi}/dt = F(\widehat{\xi}, \nabla)$, but I am not sure. For this I should derive the equations used in the spectral method, so I have to study more about it first; in the code FFT is used in several steps, so the exact form of the spectral equations is not completely clear for me. Thus, I am not sure how to compute the generator $\mathbf{T}$ either. Let me know if you have any advice for this.

2012-04-25 Predrag Whatever Adams-Bashforth integration are your state space coordinates. The FFT must be used in the stream-wise direction - when you are in the Fourier representation, use this to implement a rotation on each mode separately.

now in CB

For the one-parameter rotation group SO(2) acting on a smooth periodic function $u(\phi + 2\pi) = u(\phi)$ defined on domain $x \in [0, 2\pi)$ we can be explicit. The state space matrix representation of the SO(2) rotation $g(\phi)u(\phi) = u(\phi+\phi)$ by angle ϕ is block-diagonal, acting on the mth Fourier coefficient pair (a_m, b_m) in the Fourier series,

$$u(\phi) = a_0 + \sum_{m=1}^{\infty} (a_m \cos m\phi + b_m \sin m\phi) \ , \tag{4.1}$$

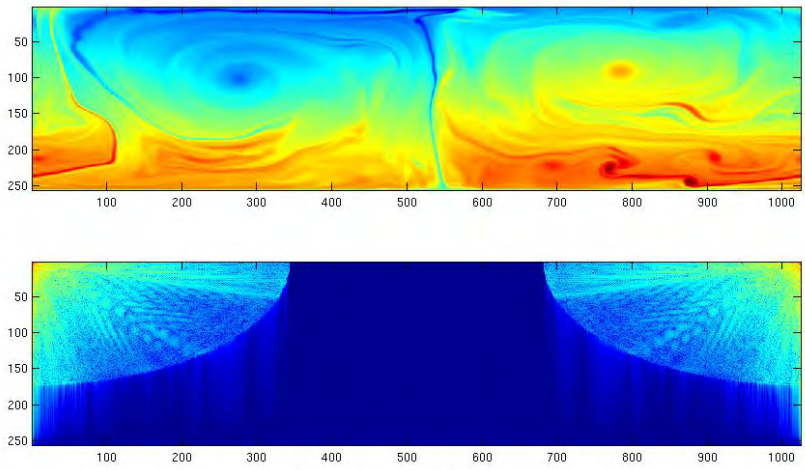

Figure 4.1: (top) Vorticity field. (bottom) Spectral representation ($ln(1 + abs(\xi))$). Note that some frequencies are just the complex conjugate of others.

by multiplication by

$$g^{(m)}(\phi) = \begin{pmatrix} \cos m\phi & \sin m\phi \\ -\sin m\phi & \cos m\phi \end{pmatrix}, \qquad \mathbf{T}^{(m)} = \begin{pmatrix} 0 & m \\ -m & 0 \end{pmatrix}. \quad (4.2)$$

In complex representation the shifts along the streamwise periodic direction z is given by

$$\vec{u}' = g(\phi, \ell)\vec{u} : \qquad \vec{u}'_{nkm} = \vec{u}_{nkm}\, \mathrm{e}^{-\mathrm{i}(m_0 m\phi + \alpha k \ell)}, \quad (4.3)$$

The SO(2) group tangent to state space point a within the mth invariant subspace is

$$t^{(m)}(a) = m \begin{pmatrix} b_m \\ -a_m \end{pmatrix}. \quad (4.4)$$

2012-04-25 Predrag You might want to form a Slicers (Slashers? a word we have not misused yet) Anonymous Support Group with Luis - he is supposed to doe exactly the same PDE slicing as you, except his symmetry is $E(2)$ Euclidean group. In his case I suggested that he does not touch the code, but post-process by turning the full space trajectory into the slice by finite angles.

2012-04-29 Sebastian I have been having a bit of trouble figuring out how to calculate the moving frame for each point. However, I think I am close to make it. Here is how I have been trying to do it: I have been using the postprocessing approach converting the vorticity output from the model back to spectral space with a fast sine transform for Y and a fast fourier transform for X (I think this is how it's done in Annalisa's code). The results of the transform are shown in figure 4.1.

This means that the vorticity can be expressed as: [1]

$$\xi(x,y) = \sum a(l)_k e^{-2i\pi kx/M} \tag{4.5}$$

So as stated in ref. [4], $g(\phi) = diag(e^{-2\pi ik\phi/M})$ and $\mathbf{T} = diag(-2\pi ik/M)$.

Now, the slice condition is given by $g(a_{kl}^T\phi(t))^T\mathbf{T}\hat{a}'_{kl}$, so I express the matrix as a vector:

$$a_{kl} = \begin{pmatrix} a_{11} & a_{12} & \cdots & a_{1N} & \cdots & a_{MN} \end{pmatrix}^T \tag{4.6}$$

and carry out the slice condition, which looks something as:

$$\begin{pmatrix} a_{11} \\ a_{12} \\ \cdots \\ a_{1N} \\ \cdots \\ a_{MN} \end{pmatrix}^T \begin{pmatrix} e^{-2\pi i\phi/M} & 0 & \cdots & 0 \\ 0 & e^{-4\pi i\phi/M} & \cdots & 0 \\ \vdots & \ddots & \ddots & \vdots \\ 0 & 0 & \cdots & e^{-2N\pi i\phi/M} \end{pmatrix} \tag{4.7}$$

$$\cdot \begin{pmatrix} -2\pi i/M & 0 & \cdots & 0 \\ 0 & -4\pi i\phi/M & \cdots & 0 \\ \vdots & \ddots & \ddots & \vdots \\ 0 & 0 & \cdots & -2N\pi i/M \end{pmatrix} \begin{pmatrix} \hat{a}'_{11} \\ \hat{a}'_{12} \\ \cdots \\ \hat{a}'_{1N} \\ \cdots \\ \hat{a}'_{MN} \end{pmatrix}^T = 0 \tag{4.8}$$

which after carrying it out gives me something as (but I have to check the algebra):

$$g(\phi(t))^T a_{kl}^T T \hat{a}'_{kl} = \sum_{n=1} \left[ne^{-in\phi} \left(\sum_{m=1} a_{mn}\hat{a}'_{mn} \right) \right] = 0 \tag{4.9}$$

I guess the next step would be to apply a Newton-Raphson to (4.9). However, I am not sure how this would work, as the equation have quite a large amount of terms, and has also an imaginary component. Let me know if you have any advice for this.

Note: I will check the algebra tomorrow again; most likely I made an embarrassing amount of mistakes while writing this. It is to late now.

2012-04-29 Predrag You rotate only the fast Fourier transform for X, there is no translational symmetry in the Y direction.

A vector is a vector, both in space and in Fourier space, so I do not see why a_{mn} became a matrix. Hope this helps (real form - complex is even simpler):

Consider the general action of an SO(2) symmetry on arbitrary Fourier coefficients of a spatially periodic function. Substituting this into the slice condition

[1] Predrag: $a(l)_k$ stands for $a(y,t)_k$, i.e., coefficients carry spanwise and time dependence? Or what is this l?

and using $g^{(m)}(\phi) = \cos(m\phi)\,\mathbb{1}^{(m)} + \sin(m\phi)\frac{1}{m}\mathbf{T}^{(m)}$, we find that

$$\langle e^{-\phi\mathbf{T}} a|t(\hat{a}')\rangle = \langle a|\sum_m \left(\cos(m\phi)\,\mathbb{1}^{(m)} + \sin(m\phi)\frac{1}{m}\mathbf{T}^{(m)}\right) t'\rangle$$
$$= \sum_m \Big(\langle a|\mathbf{T}^{(m)}\hat{a}'\rangle\cos(m\phi) - m\langle a|\,\mathbb{1}^{(m)}\hat{a}'\rangle\sin(m\phi)\Big) = 0\,. \qquad (4.10)$$

This is a polynomial equation, with coefficients determined by $\langle a|\mathbf{T}^{(m)}\hat{a}'\rangle$ and $\langle a|\,\mathbb{1}^{(m)}\hat{a}'\rangle$, as we can see by rewriting $\cos(m\phi)$, $\sin(m\phi)$ as polynomials of degree m in $\sin(\phi)$ and $\cos(\phi)$. Each phase ϕ that rotates a into any of the group-orbit traversals of the slice hyperplane corresponds to a real root of this polynomial.

It is fast - just a dot product, and as ϕ dependence is only in the group element, the $d/d\phi$ derivative you need for Newton. Complex Newton formula is the same as for real functions, thanks to analyticity (analyticity assures that complex derivatives make sense).

2012-04-30 Sebastian I do not understand why the transpose gets replaced by a complex conjugate. I see in matlab what you mean by the transpose of the matrix. But why does the complex conjugate gets involved in the transpose.

2012-04-30 Predrag If you are going to work in complex representation, the norm of a complex vector $a \in \mathbb{C}^d$ is $\| a \|^2 = a^* \cdot a$, and $(ga)^* = a^* g^\dagger$, where $g^\dagger$ is the hermitian conjugate = transpose + complex conjugate.

2012-04-30 Predrag Before getting into the Newton for this - make sure that your $g(\phi)$ applied to a baroclinic state a does shift it by ϕ, i.e., $g(\phi)a$ is the same $2D$ picture, but shifted by ϕ.

2012-04-30 Sebastian I have made a Matlab code that shifts the image by a ϕ. Using $g(\phi) = diag(e^{-2\pi i k\phi/M})$. Looks as expected when converted back to physical space.

2012-04-30 Sebastian I reshape a matrix into a vector as Matlab's FFT works by columns. What I have is a matrix that represents a vorticity field [2] so what I do is to make a Fast Sine Transform (FST) in Y and a FFT in X. This is something similar to performing a 2D FFT. But to move all the fourier coefficients in X, I reshape everything again as a vector. And then carry out the slicing condition (all this in paper, in Matlab I have go up to the FFT transform representation). So I think this would be equivalent only to a shift in X.

Vector turns out to be huge, 262144 dimensions for complex numbers; so really is like 524288 dimension. But a bit less than half of them are just complex conjugates.

[2] Sebastian: which actually is given as a vector from Annalisa's code, but I reshape it into a matrix before doing anything in matlab

The term $a(l)_k$ means actually $a(l,t)_k$. I use it just to emphasize that the transform in x, which is related with k, is performed after a FST is made on the data for the y direction. The subindex l is related to y. So $a(l)_k$, or perhaps better to write a_{lk}, is a matrix (as shown in figure 4.1), that I have to reshape to rotate into the slice. But I am not really sure why you think it should be a vector.

2012-04-30 Predrag Not sure why things got so huge? No point using Matlab for this - it is fast and simple writing a dot product in C++ or Fortran. This is Annalisa's department.

2012-04-30 Sebastian I think the general procedure of what I did yesterday is OK. I have been making the calculations this morning again. I believe is similar to what you did in (4.10), just that in complex space. By the way, how do you get $e^{-\phi\mathbf{T}}$ to multiply t' directly? Is it because there should be a transpose in $e^{-\phi\mathbf{T}}x$?

2012-04-30 Predrag To view just the project (without this blog) toggle the `boyscoutfalse` switch, towards the top of `siminos/baroclinic/BrCv12.tex` file.

now in CB

2012-04-30 Sebastian How do you show that $\hat{a}'^{\dagger}\mathbf{T}\hat{a}' = 0$?

2012-04-30 Sebastian, Predrag Unitary transformations preserve the magnitude of a complex vector $\| a \| = \| g(\phi)a \|$, so $g^{\dagger}g = 1$. Expanding the norm to leading order in ϕ $\langle(1+\phi\mathbf{T})|(1+\phi\mathbf{T})\rangle$ shows that the generators are antihermitian, $\mathbf{T}^{\dagger} = -\mathbf{T}$, and from that it follows by complex conjugation of the dot product $a^{\dagger}\mathbf{T}a$ that $a^{\dagger}\mathbf{T}a = 0$ for any vector $a \in \mathbb{R}^d$.

To evaluate the slice condition for unitary groups,

$$\frac{\partial}{\partial\phi} \| a - g\hat{a}' \|^2 = 0\,, \tag{4.11}$$

start by expanding

$$(a - g\hat{a}')^{\dagger}(a - g\hat{a}') = \| a \|^2 - \hat{a}'^{\dagger}g^{\dagger}a - a^{\dagger}g\hat{a}' + \| \hat{a}' \|^2$$

so

$$\begin{aligned} \frac{\partial}{\partial\phi}(a - g\hat{a}')^{\dagger}(a - g\hat{a}') &= -\frac{\partial}{\partial\phi}(\hat{a}'^{\dagger}g^{\dagger}a + a^{\dagger}g\hat{a}') = -2\,\mathrm{Re}\left(a^{\dagger}\frac{\partial g}{\partial\phi}\hat{a}'\right) \\ &= -2\,\mathrm{Re}\left(a^{\dagger}g\mathbf{T}\hat{a}'\right)\,. \end{aligned} \tag{4.12}$$

Substitute $a = g\hat{a}$. [3] This yields the *slice condition* for unitary groups:

$$\mathrm{Re}\,(\hat{a}^{\dagger}\mathbf{T}\hat{a}') = 0 \tag{4.13}$$

One uses this condition for Newton-Raphson determination of $\hat{a}$.

[3] Predrag: This is OK for abelain groups, as along the way I assumed $g\mathbf{T} = \mathbf{T}g$, but have to redo it more carefully for nonabelian groups.

2012-04-30 Sebastian I tried to run the model changing the resolution, but results do not look good. Not much happened, energy did not traveled up scale. Small scales are important. I think the simulation starts looking good from 512×128 so I might change to that one. But there is always the chance that I did not change some parameter in the simulation needed when changing scales. I would have to check with Annalisa.

2012-04-30 Sebastian Not sure $a^\dagger \mathbf{T} a$ vanishes, although it is antihermitian it is a diagonal matrix. I think the correct answer is:

$$a^\dagger \mathbf{T} a = -\sum_{l=1} \sum_{k=1} ik \|a_{l,k}\|^2 \tag{4.14}$$

Let me know if I am missing something.

2012-05-01 Predrag Maybe elementary, student Ortega. Take $[1 \times 1]$ antihermitian matrix $\mathbf{T} = \mathrm{i}$. It's diagonal, right. And $\mathbf{T}^\dagger = -\mathrm{i}$. If we did this as SO(2) there would be no confusion, but with U(1) one tends to get confused. BTW, there is no sum on l in (4.14) - it vanishes for every value of l separately.

$a^\dagger \mathbf{T} a = (x - \mathrm{i}y)\mathrm{i}(x + \mathrm{i}y) =$

2012-04-30 Sebastian Ok. So a'+Ta' vanishes? I do not see it. I can go by your office and tell you how I derive it, maybe you can tell me where I went wrong. The sum in l is an artifact of how I derived things.

2012-05-1 Sebastian Finish writing a very quick draft of the non linear section.

2012-05-1 Sebastian Did some tweaking for the final project. Now it is in final form. I did not have time to check all equations, but I guess they are ok. I will go after Thursday trough the derivation of (1.49) and run the algorithm to see what happens.

I think it turn out ok. I like the final result. Let me know what you think. As usual comments are greatly appreciated.

2012-05-4 Sebastian I have been trying to implement the slicing condition of the term project. Newton method converges and it is quite fast, even for the 1024x256 runs. However, it always converges very near the initial guess, so that something is wrong. I was also thinking of how is one to implement the chart border condition given that we are dealing with complex numbers.

2012-05-04 Predrag If you are going small steps in time, this sounds right - the in-slice trajectory will be close to the full space trajectory. You just have to be sure that all points on it satisfy the slice condition.

2012-05-04 Sebastian Let me know if you have any advise for any of these points.

2012-05-04 Sebastian I spotted some things I can correct in my final work (minor changes), let me know if changes are still allowed.

2012-04-30 Predrag Keep editing and improving it - I can always post improved version on ChaosBook.org/projects. As far as I am concerned, this project is not over until either the fat lady sings, or you slice the baroclinic instability.

2012-05-05 Sebastian Not sure if ϕ is correct. I am using all the time steps of the simulation. If I start at $\phi = 0$ then the algorithm converges to something near 0.1 for the next step; but from looking at the simulations, if the drifting where to be removed, I think ϕ should be around 50 as the transformations are made using $g = \text{diag}\{e^{-2i\pi k\phi/N}\}$ where $N = 1024$. Any number less than unity for ϕ makes no sense.

2012-05-05 Predrag To isolate the problem, maybe sidestep the integrator, replace it by any instantaneous state that you shift using the translation operator (instead of integrating the PDEs). That is a mock-up of a relative equilibrium, and your Newton should make it stationary in the slice.

2012-05-05 Sebastian The sidestep approach should be a good test. I will also try that.

2012-05-05 Sebastian I use (1.49) for the slice condition in Newton Method. But I am not sure how to implement the chart border condition for complex vectors. I will work something out. In the moment I am calculating the real part of the condition.

2012-05-05 Predrag There is only one shift ϕ to compute - it fixes both the real and imaginary parts of the U(1) transformation. The dot product is the usual $L2$ one, in the streamwise direction

$$\|a - a'\|^2 = \langle a - a' | a - a' \rangle = \frac{1}{L} \oint dx \, (u - u')^\dagger \cdot (u - u') \,. \tag{4.15}$$

2012-05-05 Sebastian I have been thinking about the reason my post-processing slicing does not work. I went over the code and derivation today, but couldn't find what is wrong with it. So I think it is not an implementation issue but something else. Maybe in this case (after the FFT is used), it might not be correct to regard the moving frame as continuous variable; as the rotation of the FFT only makes sense (and only works) when the moving frame is an integer (ϕ in (1.49)). This way, we might need a discrete version of the Newton-Raphson algorithm.

I will search for an algorithm for this; although it should be easy to create one from scratch; we just have to evaluate ϕ in (1.49) from 1 to 1024, and see where the values goes from positive to negative. If we select a good initial value for (1.49), and if we are lucky enough, then it should work. We won't be able to find a value that makes (1.49) zero, but this is a resolution issue. Note also that we do not always need to evaluate ϕ in (1.49) form 1 to 1024. With a good initial guess fewer points should be necessary.

now in CB

2012-05-05 Predrag Mhm - I have been wondering about this since 1993, when Eckhardt and I [58] worked out how to quotient discrete symmetries. There you

learn that if you can cut a 'pizza' into n equivalent slices, you should work in a single sliver, or fundamental domain. I tried to quotient SO(2) as a limit $n \to \infty$ of discrete cyclic group symmetry Z_n (in your case $n = 1024$), and in retrospect I believe it was a wrong path that kept me from doing the right thing (slicing) for many years. The problem is that in the discrete quotienting you make the reduced state space smaller (by replacing the full state space by a sliver) but the dimensionality of the space remains the same. In reduction of continuous symmetries you decrease the dimension of state space by one, for each continuous symmetry parameter. I do not see how one would get to this $\lim_{n\to\infty} Z_n = SO(2)$ limit by the fundamental domain approach. [4]

I think what you should do is keep ϕ continuous, and interpolate, meaning that in the Fourier rep you shift by the continuous phase, and then FFT back to space; result will not be $j/1024$ shift but something in between.

now in CB

2012-05-05 Predrag We have the same problem in slicing experimental data - it is digitized, and the slice condition will not respect the discrete pixel size, so sliced video has to be re-digitized. As this can be done as post-processing, I see no danger of introducing numerical errors into the data set.

2012-05-07 Sebastian I implemented a discrete Newton-Raphson method and it seems to work. I think I have sliced baroclinic instability. Of course, I have to think more about the chart border condition. I will upload the code at night (I don't have my laptop in the office).

2012-05-07 Predrag to Ashley Do you understand why one would have a *discrete* Newton-Raphson? Do not even know what it means... In your pipe slicing ϕ is continuous, right?

2012-05-07 Sebastian Here is the first animation of sliced baroclinic instability: [5]

../movies/BaroclinicSlice.avi.

As expected, the slice seems to be useful only for a limited time. But ignore the chart border condition in the moment. It might be correct, but I have to check.

2012-05-07 Predrag to Sebastian Slicing does seem to stop the flow from drifting, but otherwise not much simplification - it will be hopefully more striking once you start plotting trajectories in the state space.

The chart border condition (1.50) is

$$\langle t(\hat{a}^*)|t'\rangle \;=\; 0\,.$$

I'm bothered by 10^{-5} magnitude of whatever you are plotting. How about plotting just the cos of the angle between the two tangent vectors,

$$\cos\theta = \frac{\mathrm{Re}\,\langle t(\hat{a}^*(t))|t'\rangle}{\|t(\hat{a}^*(t))\|\;\|t'\|}\,, \tag{4.16}$$

[4] Predrag: to Predrag - copy this to pipes/blog

[5] Predrag: the animation is not in the repository to save space - if you want to have a look, I can place it in the DropBox.com

using (1.51) and (1.52)? Whenever this goes through zero, $\hat{a}(t) = \hat{a}^*(t)$, you have fallen off the chart border. It should be doing it smoothly, as the template is arbitrary, so there is nothing special for the full state space trajectory happening at that instant. Plot $\|t(\hat{a}(t))\|$ as well; it should also vary smoothly, and *not* get very small: if it does, alert me - it indicates that you the trajectory is passing very close to an invariant subspace, and physically that is very important.

Ashley is measuring the same thing for the pipe flow, you two might want to compare experiences.

2012-05-07 Sebastian I implemented something for this a few days ago, but I have to check. What is implemented is different from (1.51); and I didn't spend enough time in the derivation so most likely it is incorrect. I will plot the cos of the angle and $\|t(\hat{a}(t))\|$ once I have the implementation. I am uploading the code I used. That is, the following three files:

- `Slice.m`. Main file.
- `sliceFunction.m`. Function to calculate (1.49).
- `PlotSlice.m`. To make the movies.

Newton-Raphson implementation is just a couple of lines in `Slice.m`. It is very similar to the continuous version, just that everything is evaluated in integer values of ϕ in (1.49). A centered finite difference equation is used to evaluate the derivative of (1.49).

2012-05-07 Sebastian Not sure where Ashley's notes are in SVN. Let me know where to find them. It would be great to compare.

2012-05-07 Predrag There are no notes other than our paper [4] [click here]. Really do not understand why Newton would become discrete...

2012-05-09 Sebastian I implemented the correct version of the chart border condition.

../movies/BaroclinicSlice1.avi.

The equations I used where similar to the ones you wrote down in the project, just a couple of squared terms here and there. I think now we should start charting the state space by defining more slices. I will start thinking about how to do it.

2012-05-09 Predrag "similar" is not good enough - please keep correcting them and describing what you are doing precisely, otherwise how am I to help? And how is anybody to reproduce your results?

$[-4, 2] \times 10^{-13}$ does not look like cos as defined in (4.16). What state is used as a template? If it is the first frame, that looks like a nice choice. What happens as you fall off the chart border? I'm not noticing anything screwy in the sliced video evolution, in it does not look much different from [2012-05-07] movie. You see something qualitatively different?

So far, you have removed the drift, which is nice, but I am hoping for much more. Videos are quickly not useful. You really have to go to state space to appreciate

slicing. Please study the state space tutorial, then we can try to implement it here. Annalisa did start looking at the energy/dissipation plots, but I find state space visualizations much more powerful.

2012-05-09 Predrag Best to stick movies in the DropBox.com - they clog up email fast.

2012-05-09 Sebastian I have also been thinking in how to start exploring implications in Tropical Weather and Climate. I sent an email to Peter with possible research work for my Phd a couple days ago; it would be great to get your comments on this (emailed pdf). Of course, I still have to meet with Peter to talk about this and focus the idea.

2012-05-09 Predrag I do not know Peter (other than when you see him, tell him that Predrag still owes him a colloquium dinner) but Professors can be finicky about what their students do. I would love to collaborate on something Peter thinks might be useful to climatology - and I liked the chaos project his student Carlos D. Hoyos did. Best to ask Annalisa for advice. You can put the tex file of this into repository and we can maybe edit it a bit to make a stronger climatology case.

2012-05-09 Sebastian I think Newton-Raphson becomes discrete as there is no meaning for something as a non-integer moving frame when you think about it in terms of the FFT. If one tries to plot a shifted imaged using non-integer moving frames in (1.45) the resulting image after the inverse transformation gets distorted, if one uses integer values the image is just shifted. So maybe when non-integer values are used to calculate 1.49 the values are affected by this resolution issues.

When ones thinks in terms of finding the shifted state $(g(\phi)a)$ which best compares to the slice (a') for a given time, there is no sense in considering one for which ϕ equals something as 23.43 (or any other non-integer value), there is simply no state (image) defined there, one needs to compare those values where ϕ is an integer, for only there we have states (images).

I would go again trough the implementation of the chart border again, then I will upload the files and equations. I will go trough state space tutorial also.

2012-05-09 Sebastian Focusing my thesis in predictability in the tropics might be the right path for my Phd. Right now I am working in convectively coupled waves in the tropics, and there are some models one could use to explore dynamics, or one could also explore data. I will think more about this.

2012-05-09 Ashley to Sebastian Firstly, hi!

It looks like there are a couple of questions regarding notation. Please take a look at the first couple of paragraphs of §2.3 in [4] [click here], only about 10 lines. Note that ϕ is a length or angle and is therefore continuous, it can take any value. Applying a shift in the Fourier space, the new coefficients are $b_m = \mathrm{e}^{-\mathrm{i}m\phi}a_m$, which can be calculated to numerical precision. There is no distortion. Perhaps

you are thinking of the data on a discretised grid. Don't worry about the grid — once you have the Fourier coefficients you can evaluate the sum on as many spatial points as you like.

The dot product of two vectors is a real number, and the inner product is a normalised integral over the dot products. It should therefore also be real. I suspect your taking the real part is a numerical artifact that may be related to the condition that $a_m = a^*_{-m}$. In my case I only store coefficients for $m \geq 0$, then to evaluate the norm I get the contribution for the $m = 0$ mode, then double the real part of the contribution from the $m > 0$ modes. The complex part would have cancelled if I did the actual sum over negative and positive m.

2012-05-11 Sebastian to Predrag The state which is used as the template is the first frame. I am not really sure what happens when it fall off the borders. From the animations I sent you it seems that not much happens, the drift keeps getting removed; as you stated, I have to go to state space to appreciate what happens. I will start by plotting the first harmonics of first layer.

2012-05-11 Predrag to Sebastian Absolutely *no* harmonics, please - that is obsolete, 20th century way of looking at the state space. Please use Gibson and mine physical coordinate frames, as described in the tutorial and refs. [3, 59, 4]. You will be a century ahead of competitors, as it looks like no-one among plumbers and weathermen has grasped that this is something they do not understand and do not do.

2012-05-11 Sebastian to Predrag There is nothing qualitatively different in the movie either, basically is the same movie, only now the chart border condition is calculated differently.

I got different results for (1.51) and (1.52). For the former I got:

$$\|t(a)\|^2 = \langle t(a)|t(a)\rangle = \frac{4\pi^2}{N^2}\sum_{k=0}^{N-1}\sum_{l=0}^{M-1} k^2\,\overline{a_{lk}}a_{lk} \tag{4.17}$$

and for the latter:

$$\langle t(\hat{a}^*)|t'\rangle = \hat{a}^\dagger \mathbf{T}^2 \hat{a}' = \frac{4\pi^2}{N^2}\sum_{k=0}^{N-1}\sum_{l=0}^{M-1} k^2\overline{a_{lk}}a'_{lk} \tag{4.18}$$

I use this equation in the implementation. I had a sign difference in the previous code, and forgot to take square roots of (4.17); hence the strange numbers for $\cos\phi$. I think it is better this time (see figure 4.2)

2012-05-11 Predrag That now looks about right.

- At $t = 19$ and 95 you are crossing the chart border, so your slice condition determined ϕ should jump discontinuously, if we are doing the right thing [22] I think it should jump by π.

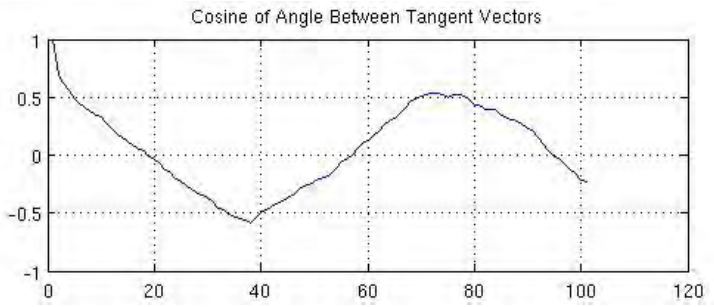

Figure 4.2: Chart border calculated as in (4.16).

- Why does the curve look so kinky? Because of your discretization by 1024 (that I pray is going away soon)?
- what's going on at $t = 1$?
- what's going on at $t = 38$ and 55?

It could be that the kinkiness is real, as you have a huge Reynolds number, i.e. structures on scales much smaller than the channel width.

2012-05-11 Sebastian to Predrag My impression from the state space tutorial is that we first need to find some relative equilibria to make really striking visualizations. The only one we have right now is the trivial one, far away from the interesting dynamics. So I think the first step is to search for them looking at Annalisa's energy/dissipation plots. For this I think we need good charts of the dynamics, so I will try to define more slices. Please let me know if this is the case.

2012-05-11 Predrag I believe that at this stage exact relative equilibria are only a distraction. You have to pick some typical snapshots of the flow as your templates, like you do at $t = 0$, to make really striking visualizations. No need for exact solutions. This is important, because I want experimentalist to slice their data as well, and they will never have any exact solutions.

2012-05-11 Sebastian to Ashley Hi Ashley!

I did used a different notation that the usual one in Chaosbook. I think ϕ (as in (1.45)) is continuous in the physical sense, only that it has to be regarded as discrete when one tries to implement it. When I tried a continuous Newton-Raphson for this it failed to converge to something meaningful. Maybe if I had followed the convention and used something as $\phi' = 2\pi\phi/N$ to iterate, then I would have not had this problem.

Regarding the dot product in equation (1.52) I actually got something as in (4.18) (I will correct (1.52) afterwards). In the code I only consider the real part of (4.18), however the imaginary component is not zero. I think it should not vanish

in general. But I might be missing something, please let me know why you think it should vanish.

I will fix the code to take advantage of the $a_m = a^*_{-m}$ property.

2012-05-11 Predrag After you have implemented the $a_m = a^*_{-m}$ property, replot figure 4.1. Your 'spectral representation' should be just the right half, no reflection symmetry.

2012-05-14 Ashley to Sebastian There is no need to worry about spatial discretisation, as shifts by ϕ and inner products can all be calculated from the data in Fourier space.

The 'conjugate-symmetric' property $a_m = a^*_{-m}$ ensures that the variable a is real, as $a_m e^{im\phi} + a_{-m} e^{-im\phi}$ is then a real contribution in the Fourier sum. Now, if a and b are real variables, then their innerproduct must also be real. Most FFT libraries only return half the data for the real→complex transform (a_m for $m \geq 0$) and cite the conjugate-symmetric property for the rest. I'm not sure why you have the rest of the data present.

I've scanned through the notes above, but I'm not sure what your index l is on some variables. If you have a double-Fourier transform, then the conjugate symmetric property is $a_{km} = a^*_{-k,-m}$.

2012-05-17 Sebastian to Predrag and Ashley I have been trying to implement the slice condition taking advantage of the FFT symmetry (i.e. using only the FFT coefficients from 0 to N/2). I manage to do so but I had to use a bunch tricks (i.e. defining a plausible interval for the moving frame, making it always positive and between 1 and 1024, and adding some random kick when the iteration gets stuck in an infinite loop; all of these can be seen in the uploaded code); they kind of make sense. I did this for a continuous version of the Newton-Raphson algorithm; here it did not seem to be an issue. The drifting gets removed, however the slice and chart border conditions change dramatically, and are not as smooth any more.

The implementation was done taking only half of the values of the transform to calculate (1.49), (4.17), and (4.18). After all, these first $N/2+1$ coefficients are the only ones really independent, and the rest are just complex conjugates. So maybe I just need to consider these to build the state space vectors:

$$\mathrm{Re}\,(\hat{a}^\dagger \mathbf{T} \hat{a}') = \mathrm{Re}\left(\frac{-2\pi i}{N} \sum_{k=0}^{N/2} \sum_{k=0}^{M-1} \overline{a_{lk}} a'_{lk} k e^{\frac{-2\pi i k}{N}\phi} \right) = 0 \tag{4.19}$$

$$\|t(a)\|^2 = \langle t(a)|t(a)\rangle = \frac{4\pi^2}{N^2} \sum_{k=0}^{N/2} \sum_{l=0}^{M-1} k^2\, \overline{a_{lk}} a_{lk} \tag{4.20}$$

and

$$\langle t(\hat{a}^*)|t'\rangle = \hat{a}^\dagger \mathbf{T}^2 \hat{a}' = \frac{4\pi^2}{N^2} \sum_{k=0}^{N/2} \sum_{l=0}^{M-1} k^2 \overline{a_{lk}} a'_{lk} \tag{4.21}$$

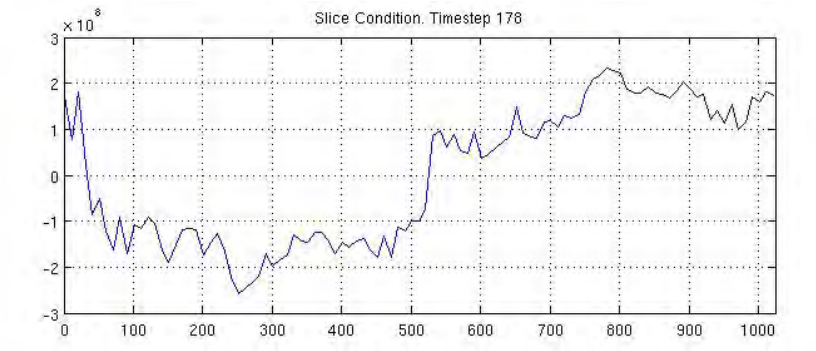

Figure 4.3: Graph of (1.49) using half of the coefficients.

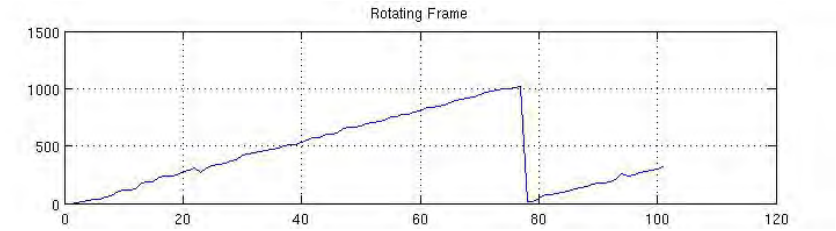

Figure 4.4: Calculated moving frame using half of the coefficients. The jump in the moving frame is due to something I impose in the code (my moving frame is limited to change between 0 and 1024). I think my implementation might remove jumps of 512 in the moving frame (equivalent to π in the usual definition) when they occur, as it limits the search area for the zeros of (4.19)

However, I ran into serious difficulties, so I think I am doing something wrong. In particular, the chart border condition makes no sense. It starts at 1 (which is expected as I start the iteration at the same time step corresponding to the slice) and then just wonders around zero (see figure 4.9). In my previous implementation things where a lot more smoother (see figure 4.5), although one had to regard everything as discrete (to see why see figure 4.7). Additionally, the moving frame of both representation seems to change when looking only to a particular time step (see figure 4.6), but I should look at all the time steps to conclude about this.

I was wondering how complicated was to implement this for pipe flow, and if you ran into similar difficulties. I will keep thinking about what is wrong. Let me know if you have any advice.

Note: The new code is Slice2.m and sliceFunction2.m. I left the previous one for reference.

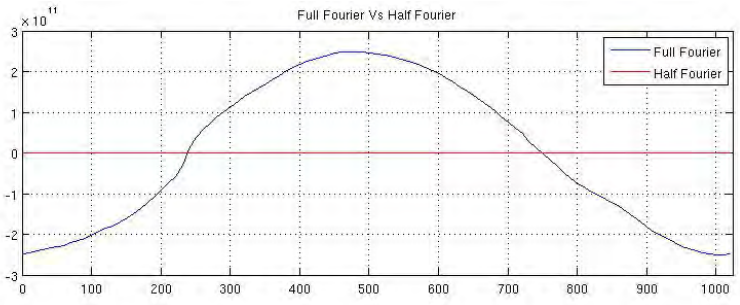

Figure 4.5: Rotating frame calculated using the full coefficients of the FFT representation (Blue) and half of them (Red)

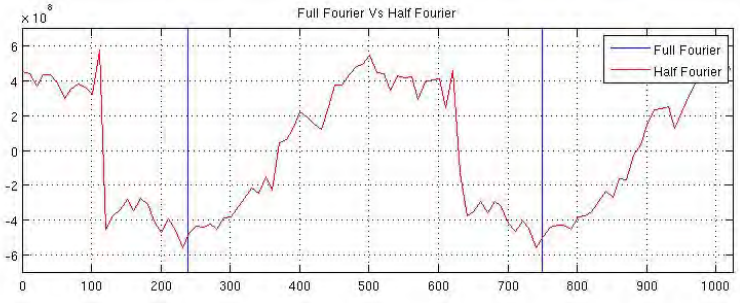

Figure 4.6: Rotating frame calculated using the full coefficients of the FFT representation (Blue) and half of them (Red)

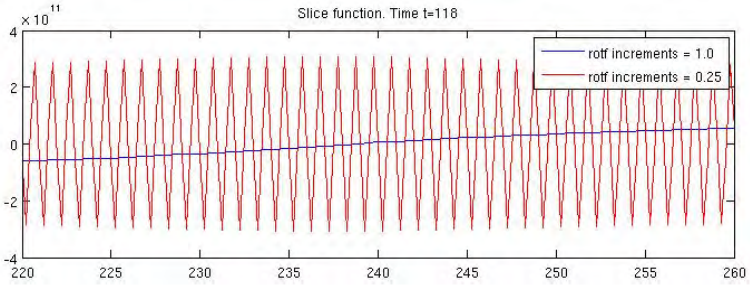

Figure 4.7: Slice function with the full fourier representation (1.49) calculated using integer values for the moving frame (Blue) and steps of 0.25 for the same variable (Red)

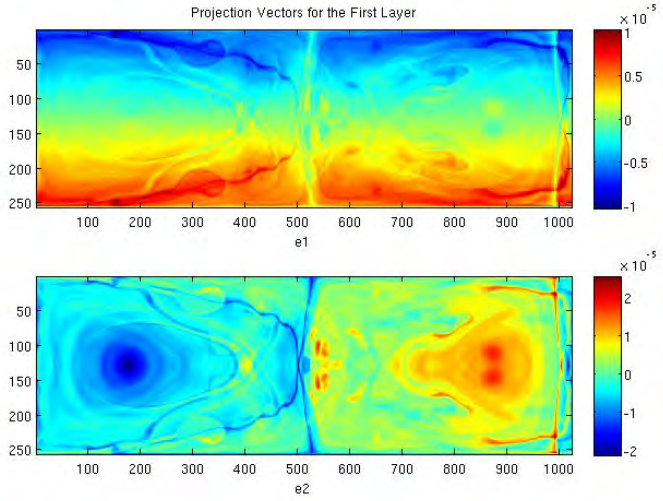

Figure 4.8: Orthonormal basis set $\{\mathbf{e}_1, \mathbf{e}_2, \cdots, \mathbf{e}_n\}$: $\mathbf{e}_1$ is the antisymmetric vector, and $\mathbf{e}_2$ the symmetric one, see (4.22). Only the first layer is shown.

2012-06-04 Predrag Here is our ultimate goal.

2012-06-04 Sebastian Great webpage. I am not sure I understand which is the ultimate goal you are referring to; but I guess great visualizations is part of it.

2012-06-04 Sebastian I think the discrete implementation had some issues with aliasing; I was using frequencies higher that that of Nyquist. Nonetheless, somehow results seemed smoother. In the DropBox uploaded movie `BaroclinicSlice2.avi` (now in Predrag's `siminos/movies/`, not in the repository) one can see the drifting is not removed as smoothly as before. So maybe a smaller time step needs to be considered. But probably is because I am missing something.

2012-06-04 Predrag We need to construct an orthonormal basis set $\{\mathbf{e}_1, \mathbf{e}_2, \cdots, \mathbf{e}_n\}$, with $\|\mathbf{e}_j\| = 1$ (using notation of sect. 2.2.1). We chose as a 'template' $\hat{a}'$ a 'prominent state of the flow,

$$\hat{a}' = \mathbf{u} = \mathbf{u}(x, y) = \mathbf{u}(x, y, t)\,,$$

an instantaneous snapshot of a steady turbulent state at arbitrary fixed time t. The spanwise reflection is a symmetry, so we can construct $\{\mathbf{e}_1, \mathbf{e}_2\}$ from the orthonormal pair of vectors

$$\mathbf{e}_{1,2} = \frac{\mathbf{u}(x, y) \pm \mathbf{u}(x, -y)}{\|\mathbf{u}(x, y) \pm \mathbf{u}(x, -y)\|}\,. \tag{4.22}$$

An example is given in figure 4.8.

2012-06-04 Sebastian I projected trajectories onto (a_1, a_2) using

$$a_j = \mathbf{e}_j \cdot u = \mathrm{Re}\left[\sum_{n=1}^{2}\sum_{l=0}^{M-1}\sum_{k=0}^{N/2} u_{lkn} e^i_{lkn}\right], \tag{4.23}$$

where $j = 1, 2$ defines the basis vector, n accounts for the layers and m for the longitudinal direction. I uploaded the results to Dropbox's Chaos folder. Of course, this might not mean much if the chart border condition in figure 4.9 is correct.

I think the movie shows some recurrences. But I am not so happy with the slicing, and I am not sure if they really mean something, as I have to figure out what is wrong with the implementation.

2012-06-06 Predrag Can you read sect. 2.2.2 and use the same names? The time steps do look too big in your current (non-orthogonalized) $\{a_1, a_2\}$ projection.

Do you understand **[2012-05-09 Ashley]**, **[2012-05-14 Ashley]** above and agree with him? Or is your Newton still discretized? Ashley (or Gibson) will help you, if you ask them.

The doctor is in (later today).

2012-06-12 Sebastian to Predrag and Ashley I fixed the names in the last post. Model geometry is drawn in figure 1.3.

Newton is now continuous. However, results looked better when it was not, and implementation was also "cleaner" (see **[2012-05-17 Sebastian to Predrag and Ashley]**); but this was probably for the wrong reasons.

I do understand and agree with Ashley. Nonetheless, I do still think that taking the real part of the result in (1.49) is necessary (as can be seen in the derivation **[2012-04-30 Sebastian, Predrag]**), and is unrelated to the FFT property $a_m = a^*_{-m}$.

Recently I tried to implement the moving frame and the chart border condition just taking into account the first $N/2$ frequencies. I did it considering them as independent coordinates and not accounting for the aliased frequencies given by the FFT for any sum; the results are not too smooth. I also tried yesterday to do it taking account of this aliased frequencies; however results do not look nice so far. Maybe, because it is not clear to me how one should proceed. For instance given the equation

$$\langle t(\hat{a}^*)|t'\rangle = \hat{a}^\dagger \mathbf{T}^2 \hat{a}' = \frac{4\pi^2}{N^2}\sum_k \sum_{l=0}^{M-1} k^2 \overline{a_{lk}} a'_{lk} \tag{4.24}$$

one could evaluate it using k form 0 to $N-1$, or form $-N/2+1$ to $N/2$ (or just from 0 to $N/2$, as I did before). I think the results will vary a lot, but maybe the second option makes more sense. I tried yesterday to implement this; and will try again today. Is this the correct way to do it?

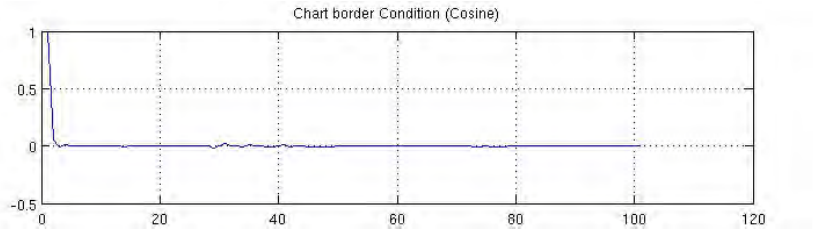

Figure 4.9: Cosine of the angle between the tangent vectors using half of the coefficients. This is calculated using (4.35) and (4.36).

I also uploaded in the DropBox uploaded movie `BaroclinicSlice3.avi` (now in Predrag's `siminos/movies/`, not in the repository). I think reducing the time step might be necessary.

I am not sure what is wrong with the slicing. I believe one should be able to slice it due to the symmetry. But maybe we need a much smaller time step, this way the slice would be valid for more steps (if figure 4.9 is correct, then the slice is only valid for the first couple of time steps). Maybe linear slices are only good for really small times in this particular simulation.

2012-05-13 Predrag It might be that the chart encompassing a given template is very small, and that your figure 4.9 is correct. Once you are gone beyond the Chart border the orientation of the tangent vector $t(\hat{a}^*(t))$ in (4.16) might be essentially random compared to the t', and in high-dimensional vector spaces two random vectors are nearly orthogonal. I would integrate from $t = 0$ to $t = 4$ in very small steps, consider in more detail what $t(\hat{a}^*(t))$ is doing (make a movie of it).

2012-06-13 Sebastian and Predrag Following up on **[2012-05-09, 2012-05-14 Ashley to Sebastian]**: Need to fix (4.14), (4.19)-(4.36), (4.23), (4.24), evaluate using k from $-N$ to N (instead of 0 to N), then use $a_m = a^*_{-m}$ and/or $a_{km} = a^*_{-k,-m}$ to prove that all dot product of vectors that you compute are real numbers (due to the reality of $u(x, y)$, with no need to impose (4.13)). In particular, (4.14) is wrong, fix it.

2012-05-13 Predrag From `BaroclinicSlice3.avi`, and the simultaneous projection on the $\{a_1, a_2\}$ (in basis of figure 4.8), it is clear that the time steps are gigantic - need to integrate in fine steps for one large structure turnover time, $\Delta t = 10 - 100$.

The situation is much more difficult than in the (very smooth) pipe flows near onset of turbulence. The picture that is emerging is a large, lumbering wall to wall structure, with very fast small vortices on top of it. Hopefully they act as noise, and smear the the state space trajectory of the large structures. Perhaps it is these vortices that make a chart in figure 4.9 so short-lived; so new thinking is needed.

Our first goal would be to find a smooth (no fine vortices) relative equilibrium solution, use it to replace figure 4.8.

2012-07-16 Sebastian I went over the implementation, and I think I had a problem with the theory but end up doing the right thing in practice. DFT is defined as:

$$\widetilde{f}_k = \frac{1}{N}\sum_{j=0}^{N-1} f(x_j)e^{-2\pi ijk/N} \tag{4.25}$$

for $k = -N/2, ..., N/2-1$. And the synthesis equation as:

$$f(x_j) = \sum_{k=-N/2}^{N/2-1} \widetilde{f}_k e^{2\pi ijk/N} \tag{4.26}$$

for $j = 0, 1, 2, \cdots, N-1$. Then the vorticity is expanded as:

$$\xi(x_j, y) = \sum_{k=-N/2}^{N/2-1} a(y)_k e^{-2\pi ikj/N} \tag{4.27}$$

and we have to consider the coefficients $a(y)_k$ for frequencies from $k = -N/2, \cdots, N/2-1$. This leads to the slice condition: [6]

$$\hat{a}^\dagger \mathbf{T} \hat{a}' = -\frac{2\pi i}{N}\sum_{k=-N/2}^{N/2-1}\sum_{l=0}^{M-1} \overline{a}_{lk} a'_{lk}\, k\, e^{-\frac{2\pi ik}{N}\phi} = 0\,, \tag{4.28}$$

but since we have the property $a_{l,m} = a^*_{l,-m}$ the imaginary numbers cancel by pairs, so that we might as well compute:

$$\hat{a}^\dagger \mathbf{T} \hat{a}' = 2\cdot \mathrm{Re}\left(\frac{-2\pi i}{N}\sum_{k=0}^{N/2}\sum_{l=0}^{M-1} \overline{a}_{lk} a'_{lk}\, k\, e^{-\frac{2\pi ik}{N}\phi}\right) = 0\,, \tag{4.29}$$

where taking the real part is just a trick to reduce computations. This is what it is implemented in `Slice2.m` and `SliceCondition2.m`. Only the factor of 2 is missing, but that would not change the results at least qualitatively. This would imply that (4.19)–(4.36), (4.23), (4.24) are correct (except for the factor of 2). But I might be missing something.

2012-07-17 Predrag Seems OK (have not checked the algebra). Weird - I did not get email about your edit. Are you getting them? (we just changed the server, there could be configuration problems).

[6] Predrag: $[-N/2, \cdots, N/2-1]$ is a strange range? Sebastian: It is the definition some authors give to the DFT (see for instance Chapter 1 of Kopriva [60]; one can get it electronically trough Gatech library webpage) probably it is done this way in order to avoid multiplying the coefficients related with $N/2$ and $-N/2$ by $1/2$. Other authors use the range $[0, \cdots, N-1]$.

2012-07-17 Predrag What is 'synthesis equation'? Sebastian: It is another way to refer to the inverse of the DFT. Predrag: Google agrees.

2012-07-16 Sebastian I will talk to Annalisa to download the code from her computer and run it in mine, or in the server, with smaller time steps. Not sure how to look for the relative equilibrium, but I guess smaller time steps are needed first.

2012-07-17 Predrag Talk to her ASAP, as she is leaving for Italy soon (for 2-3 weeks?). We have a linux server, if you need access (also to PACE cluster).

2012-07-17 Sebastian Hi Predrag. I did get the email. **[2012-07-17 Predrag]** Weird - I did not get alert of your last edit either (but get all others...).

I talked to Annalisa and have the code; she pointed out we might only need to decrease the saving intervals of the simulation and not the time-step per se.

I am now struggling to get the FFTW libraries to work on my computer. It might be easier on the server if the libraries are already installed on it.

2012-07-19 Sebastian I ran the code saving the output 10 times more frequent than before. As expected, the slicing is much more smooth now, and the chart border condition is valid for more time-steps. However the slices remain only valid for short times (see figure 4.11 (a)).

2012-07-19 Predrag Great simulation! Not having the movie but steps is quite helpful in looking at. Can you try this: instead of plotting the flow in the slice, plot the bit-by-bit differences between the two videos: it will start out white, but as you go away from the template state, it will show you only the regions where there is the fastest change; we need to understand why the small structures can drive you to the chart border.

Please check out repository `pipes` (you are sortega = baroclinic there as well), and read pipes/blog/blog.pdf starting with **[2012-05-30 Humbledt]**. You will see the same behavior for the pipe flow, but I do not believe there are small structures in that problem.

2012-07-19 Sebastian I also modified the code to redefine the slice when necessary, only to see how long are different slices valid (as have been done for pipe flow). I am uploading `multipleSlices.pdf` to dropbox (did not figure out how to make a movie here). I think what is seen is that drifting combined with the thin filaments and small vortices is the main reason for which the slices are not valid for long. I was wondering if there is possible to overcome this issue by defining something as a moving slice (along group orbits), but I am not sure how the charting would work in this case. I will keep thinking about this.

2012-07-19 Predrag As you will see in the pipes/blog/blog.pdf, I've been thinking the same way (looks like there is a rotating structure, so perhaps there is a rotating frame with charts valid for much longer times), but I think you have a better idea - we need to understand what is it that makes $\cos\theta$ go to zero so fast.

2012-07-19 Predrag Weird - when you commit, I do not get email about your edit. Do you? Forward it to me if you do. Yours is the only email that svn refuses to forward to me...

2012-07-25 Predrag So far we are measuring the distance $|a|^2 = \langle a|a\rangle$ in terms of the Euclidean inner product

$$\langle a|\hat{a}'\rangle = \sum_i^d a_i \hat{a}'_i \,, \qquad x, y \in \mathcal{M} \subset \mathbb{R}^d \,. \tag{4.30}$$

Any representation of a compact group G is fully reducible [61]. The invariant tensors constructed by contractions of $\mathbf{T}_a$ are useful in identifying irreducible representations. The simplest such invariant is

$$\mathbf{T}^\dagger \cdot \mathbf{T} = \sum_m C_2^{(m)} \; \mathbb{1}^{(m)} \,, \tag{4.31}$$

where $C_2^{(m)}$ is the quadratic Casimir for irreducible representation labeled m, and $\mathbb{1}^{(m)}$ is the identity on the irreducible subspace m, 0 elsewhere. For compact groups $C_2^{(m)}$ are strictly nonnegative. $C_2^{(m)} = 0$ if m is an invariant subspace. For SO(2) it is simply $C_2^{(k)} = k^2$, $\mathbb{1}^{(m)}$ is $[2\times 2]$ unit matrix, where k refers to the kth Fourier mode.

The dot product of two tangent fields in (1.49) is a sum of inner products weighted by Casimirs (4.31), as in (1.51)

$$\langle t(a)|t(\hat{a}')\rangle = \sum_m C_2^{(m)} a_i \, \delta_{ij}^{(m)} \hat{a}'_j \,. \tag{4.32}$$

The slice condition thus preferentially weighs higher Fourier modes. If we think of the norm as the Sobolev H^{-1} norm, it would be natural to have it as unit norm on the product of tangents, which means we should change (4.30) to

$$\langle a|\hat{a}'\rangle = \sum_m a_i \, \frac{\delta_{ij}^{(m)}}{C_2^{(m)}} \hat{a}'_j \,. \tag{4.33}$$

This would suppress higher Fourier modes, on hopefully tame the fast rotations observed by Ashley and Sebastian in pipe, respectively baroclinic flows.

Please try it! a very simple change in the slicing condition that should reduce the number of charts along short recurrent orbits.

2012-07-26 Sebastian I uploaded to the DropBox.com a movie showing the difference between the simulation on full state space and on the slices. It shows that the larger differences are in the two thin filaments that cross the domain.

../movies/BaroclinicSlice4.avi.

2012-07-27 Predrag The movie is very helpful. It shows clearly that it is the fine structure that causes charts to be small. As the Sobolev H^{-1} norm carries all of the spectral information, I think it is legal.

2012-07-26 Sebastian I think I understand the essence of what you want to say in **[2012-07-25 Predrag]** (and would like to know more about the theory; I will look in the cited reference). It appears to me that what you are proposing, in practical terms, is similar to filtering the series so that the gravest modes contribute more in the dot product.

I will work out the math for equations (1.49) and (1.51) and post it online. As a first guess I think I would get something as:

$$\hat{a}^\dagger \mathbf{T} \hat{a}' = 2 \cdot \mathrm{Re} \left(\frac{-2\pi i}{N} \sum_{k=0}^{N/2} \sum_{l=0}^{M-1} \frac{\overline{a}_{lk} a'_{lk}\, e^{-\frac{2\pi i k}{N}\phi}}{k} \right) = 0\,, \tag{4.34}$$

for (1.49) and

$$\|t(a)\|^2 = \langle t(a)|t(a)\rangle = \frac{4\pi^2}{N^2} \sum_{k=0}^{N/2} \sum_{l=0}^{M-1} \overline{a_{lk}} a_{lk} \tag{4.35}$$

$$\langle t(\hat{a}^*)|t'\rangle = \hat{a}^\dagger \mathbf{T}^2 \hat{a}' = \frac{4\pi^2}{N^2} \sum_{k=0}^{N/2} \sum_{l=0}^{M-1} \overline{a_{lk}} a'_{lk} \tag{4.36}$$

for the other equations. It seems to be a very good solution, I will implement it. I was wondering about the drawbacks, if any, of the Sobolev H^{-1} norm.

2012-07-27 Predrag The powers of k look correct.

2012-07-26 Sebastian, as a Side Note I was reading today about how the Madden Julian Oscillation (MJO) is forecasted, and its phases tracked; and I think they do something similar, to what you are proposing, using Empirical Orthogonal Functions (EOF). I believe the process is something as making composites of time-filtered series of data (20 to 60 day filter), obtaining the EOF's, and then comparing real time data to these functions to get the phase of the MJO (for this they project to a 2 dimensional space). I will learn more about this in the Fall (I am taking data analysis then). I think it would be interested to see how all this relates to the dynamics.

2012-07-27 Predrag My impression is that 'filtering' refers to deleting parts of the Fourier spectrum. Here we keep all of it, but with a weight gives less importance to high-frequency components.

now in CB

2012-07-27 Predrag Hopefully the chart border for the the Sobolev H^{-1} norm lies further out from the template than the one for the Euclidean norm: the idea is the amplitude of the higher mode in the 'baseball seam' of Fig. 7 (a) in ref. [19] is suppressed, so the template neighborhood goes further out before it hits the first group-orbit wiggle.

It seems to work for Ashley - here are two posts from `pipes/blog/`:

2012-05-22 Ashley I've played with adding templates on the fly in figure 4.10 (a). At the end of the orbit it didn't switch back to the first template — I've only permitted switching when shifts match for a closer template. The shifts often run side by side but don't cross.

2012-07-27 Ashley The Sobolev H^{-1} norm avoids need for a bunch of templates to navigate around $\mathrm{RP}_{36.72}$. See figure 4.10 (b), in particular the red line. Compare with figure 4.10 (a).

2012-07-27 Sebastian I did the slicing with the proposed weights. The equations I end up using are:

$$\hat{a}^\dagger \mathbf{T} \hat{a}' = 2 \cdot \mathrm{Re} \left(\left(\frac{-2\pi i}{N} \right)^{-1} \sum_{k=1}^{N/2} \sum_{l=0}^{M-1} \frac{\overline{a}_{lk} a'_{lk} \, e^{-\frac{2\pi i k}{N}\phi}}{k} \right) = 0 \,, \tag{4.37}$$

for (1.49) and

$$\|t(a)\|^2 = \langle t(a)|t(a)\rangle = \sum_{k=1}^{N/2} \sum_{l=0}^{M-1} \overline{a_{lk}} a_{lk} \tag{4.38}$$

$$\langle t(\hat{a}^*)|t'\rangle = \hat{a}^\dagger \mathbf{T}^2 \hat{a}' = \sum_{k=1}^{N/2} \sum_{l=0}^{M-1} \overline{a_{lk}} a'_{lk} \tag{4.39}$$

Note that I changed the sum related to k so that it goes from 1 to $N/2$. It worked (see figure **??** (b)) and now the slice is valid for much longer times, but I am not sure if we can just ignore the singularity for $k = 0$ in the slice condition. However, with the previous norm this mode was always canceled out; so it might be OK.

2012-07-26 Predrag Looks much better! In anything that has a factor of $\mathbf{T}$ $m = 0$ is removed. However, our derivation of slice starts with minimizing the distance $\| a - \hat{a}' \|^2$, so please set the $m = 0$ part of the norm to 1 until we show that is right or think of an alternative.

2012-07-26 Predrag I think we can probably make a good argument that the group manifold should be a Sobolev space $W^{1,\infty}$ with respect to group parameter derivatives - the group orbit is a smooth manifold. I have argued some time ago for Ruslan Davidchack somewhat inchoately that for Kuramoto-Sivashinsky Fourier expansion of $u(x)$ (**[2012-03-25 Predrag to Evangelos]**) that the important, nonlinearly coupled "Fourier modes contribute significantly for any magnitude not smaller than $1/m$ for the mth mode". If they do this for $k \to \infty$, the partial derivative u_x is not defined, and that would be a disaster. Which probably means for Navier-Stokes that we can demand that solutions belong to $W^{2,\infty}$ which would make it legit to use even stronger suppression of high Fourier modes, with the Sobolev H^{-1} norm diagonal $\propto (C_2^{(m)})^{-2}$.

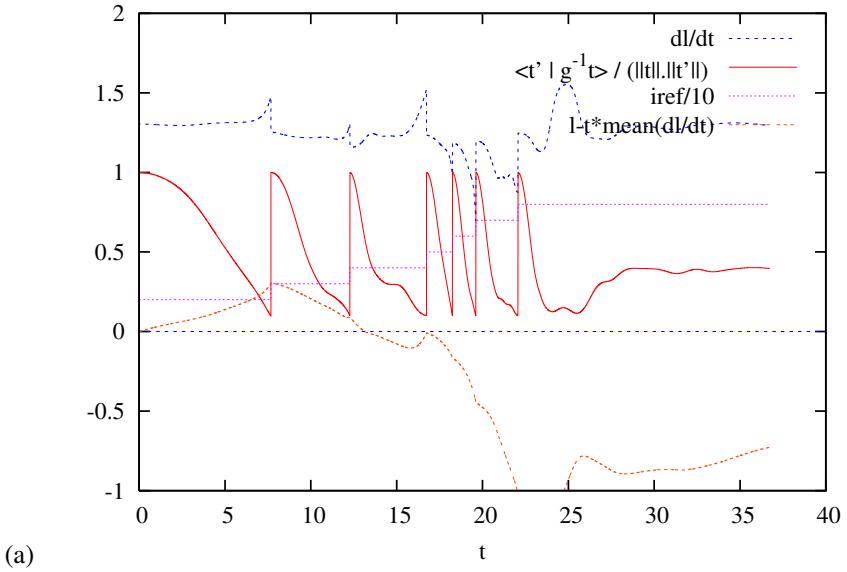

(a)

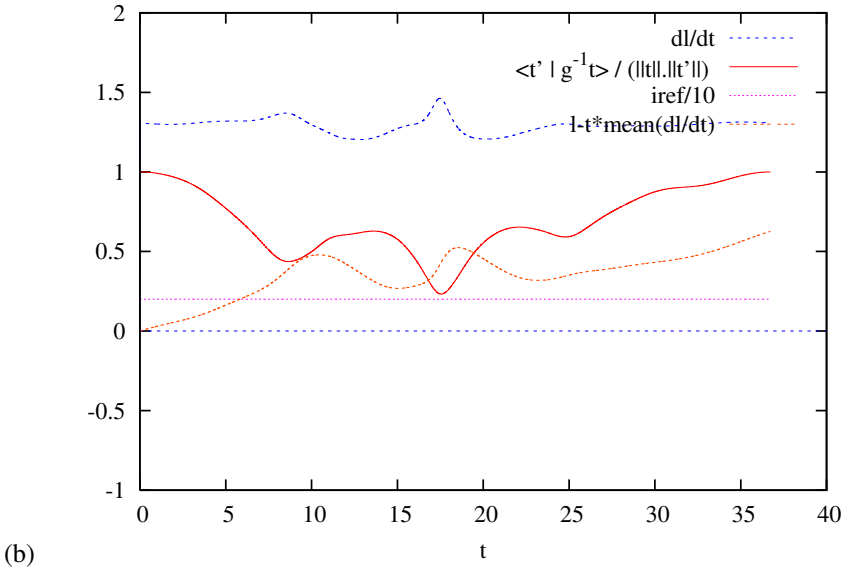

(b)

Figure 4.10: Chart border condition for the pipe flow relative periodic orbit $\mathrm{RP}_{36.72}$ discovered in ref. [4]: (a) [2012-05-22 Ashley] Tracking $\mathrm{RP}_{36.72}$ starting with $\hat{a}' = a(t=0)$ and adding new templates on the fly, whenever $\cos\psi < 0.1$. (b) [2012-07-27 Ashley] Tracking $\mathrm{RP}_{36.72}$ starting with $\hat{a}' = a(t=0)$. Just as in frame (a), except here using the Sobolev H^{-1} norm; $\cos\psi$ does not drop below 0.1.

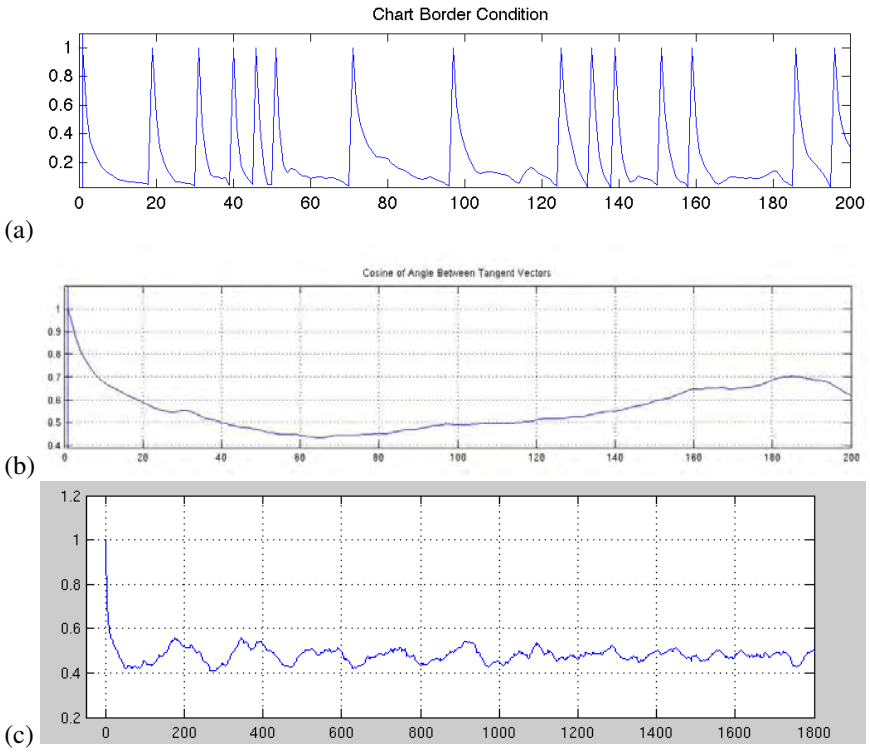

Figure 4.11: Chart border condition for the baroclinic instability [62]. The current state is used as the new template each time the cos of the angle between the two tangent vectors (4.16) is smaller than 0.05. (a) [2012-07-19 Sebastian] Using the energy norm. (b) [2012-07-27 Sebastian] Using the Sobolev H^{-1} norm (4.33). (c) [2012-08-21 Sebastian] A long run with the Sobolev H^{-1} norm.

2012-07-27 Sebastian The new norm seems to solve the problem. However I have doubts about what should we do with $k = 0$.

2012-07-27 Predrag For now, keep $k = 0$ term in the norm $= 1$. It think we need it.

2012-08-03 Predrag Jean-Luc Thiffeault reviews Sobolev norms in Sect. 3 of arXiv:1105.1101.

Can you do the movie of the sliced flow in the negative Sobolev norm, together with the norm of the difference between sliced and full state space? This time there should be no wild jumps as one seem to never get close to the chart border...

2012-08-21 Sebastian I did the slicing with the the Sobolev H^{-1} norm (4.33) for a much longer simulation. The slice seems to be valid for a really long time (see figure **??** (b)). This is kind of weird I believe; but I have not give it a good though. I have to review the norm paper for this, as probably it is an issue with the implemented norm.

2012-08-21 Predrag OK, you win - I cannot download your attachments (Beijing does things to gmail) and enter them into blog, so for this once you get email rather than a blog entry:

If we are not paying some other price for this, this might be the best news every: a single slice suffices! However, the differences between figure **??** (b) and (c) worries me: graph (b) dips much lower, and (c) is suspiciously above 0.4 for all times...

Remember, when you go back to spatial representation to reconstruct the video for reduced dynamics, you have to use the inverse of the norm (I believe). Curious what that looks like now....

2012-07-30 Sebastian I was wondering if you would like to form part of my thesis advisory committee. I am thinking in looking for periodic orbits in models of the MJO as described in *PeriodicOrbitsClimate.tex*[7] I added to the repository some days ago. As a starter I am thinking in looking at a simple Stechman [63] 2008 model (you can search for it on Majda's homepage). I am working towards implementing an spectral version of the equations.

2012-07-30 Predrag These guys have written zillion related papers since, make sure you read the relevant ones first. I have officemates in GFD Woods Hole program I'll ask about these papers.

2012-08-03 Predrag That would be great, will gladly join. Remember to apply for GFD Woods Hole Fellowship coming Fall / Spring, that would be a good place for you next summer.

2012-08-06 Sebastian I have been trying today to do the slicing for the whole simulation, however I have been ruining into some trouble with the size of the files. But I will get it done. I might also run another simulation to get more time steps.

[7] Predrag: missing *.bib entries for "Lorenz60" and "Webster72"

Regarding the applications to the MJO. I found a very simple model one might start exploring (Majda and Stechmann [64], *Nonlinear dynamics and regional variations in the MJO skeleton*). I think is better to explore this one than the one I coded up for gravity waves. As the former has nonlinearities related to advection terms; the later is simpler to analyze.

2012-08-07 Sebastian Thanks for joining! I am very happy with the committee, it would be conformed by Peter, Annalisa and yourself. Surely a great one.

I will apply to Woods Hole next summer. It seems to be a great experience. And the topics are very interesting.

The paper looks really nice. I had been a bit lost trying to find a place to study these topics. But this one seems to solve the issue. I will let you know how it goes.

2012-08-21 Sebastian Please find the presentation I gave to the group of what I want to do for the Phd. There I show results of the two models I told you about (the gravity wave and the MJO models). Due to size constraint I removed the videos. However I uploaded one to Dropbox and the other one you have it already. Let me know what you think. Note that models would need additional tweaking before being use, in order for them to be representative of the physics. And that maybe another model might be better. I wrote Professor Majda at NYU asking which he considered the best one. No answer yet, so I might write again.

I am not sure how my work dynamics will be this semester. I will be taking 2 classes, working as a TA and working on the proposal. But I am sure it will workout somehow. It will be nice to get together and set some goals.

2013-04-19 Predrag to Sebastian I've copied here for you my notes on Gritsun, from siminos/blog/ . He is geophysical, might be of interest, but read him critically.

2012-09-13 Predrag Kazantsev [65] defines some arbitrary Euclidean state space distance $r = 0.05$ as 'vicinity' and finds 90% (!) correlation with episodes in which 'barotropic ocean model' ergodic trajectory approaches his periodic orbit, whose periods range from 40 to 250 days. That cannot possibly be right - the duration of a visit to a neighborhood surely also depends on the contracting eigenvalues - if they are weakly negative, you longer in the neighborhood. Would not see that for Lorenz, as contracting eigenvalues are strongly contractive. This is not even a Kaplan-Yorke type formula, and that is easy to understand, even though his 'dimension' of a periodic orbit is Kaplan-Yorke dimension... Go figure. His 'weighted formula' for 'dimension' is in the same ballpark as what he gets from dimension $D = 5.8$ computed over 500 years of model integration.

2009-05-01 Predrag (entry in Channelflow.org) Andrey Gritsun work on unstable periodic orbits in atmospheric science sounds potentially interesting, but I have not been able to find anything to read about it. They have had an NSF grant, a number of identical conference abstracts for different conferences in 2007, 2008 and SIAM DS09, but at most one publication [66]. I am not able to get the article through GaTech library, but from the abstract I do not think he is working with

high-dimensional PDEs. There is Kazantsev work [65] from 1998, Gritsun work seems to be a continuation. Kazantsev might be worth a read for understanding what the problem is and his methodology of finding periodic orbits. Does not do this stuff any more. See **[2012-09-21 Predrag]** below.

2009-05-02 John Gibson Gritsun is working in a 200-d model of barotropic flow.

2012-09-21 Predrag OK, now I did find Gritsun [67, 68] and saved them in ChaosBook.org/library. Now have to also read Selten and Branstator [69] as well as refs. [70, 71, 72, 73].

2013-04-19 Predrag Another Gritsun paper [74]. Again with the 'escape-time weighting'. So I sent him an email:

Dear Andrey

I've been following your work with interest over the years (Sebastian Ortega, Annalisa Bracco and have been exploring the role relative periodic orbits might play in describing the baroclinic flows, have not done much so far).

I hope you do not mind a comment on your recent paper.

There once was a graduate student who was fond of running computers, but had no aptitude for mathematics. In his thesis work he wrote down a nonsensical formula for weighting periodic orbits. My colleagues and I had spent lots of time with him and that is all there is to it - a nice try, but wrong. There are many wrong formulas in physics literature and they all die quiet death, but this one is like Horatio in Hamlet - whenever you think he's dead, he gets up again and continues talking.

Can you please scratch 'escape-time weighting' from the list of things to apply to periodic orbits - you have the correct reference to Ruelle, and if you need a pedagogical textbook for non-mathematicians, you can check the derivation of the correct and only periodic orbit formula in ChaosBook.org, yours for a mouse click.

It is bit of a waste of time, but because even Kerswell used these formulas, I had to wrote about them in Remark 20.1, Alternative Periodic Orbit Theories, p. 410 of ChaosBook (version 14.4). A very brief version is in JFM Focus on Fluids to appear. I would be grateful if you point any possible inaccuracies in my remarks.

best regards, and I am looking forward to reading about more of your (for me) very interesting applications of periodic orbits to geophysical problems.

2013-07-22 Sebastian I find Chattopadhyay, Sahai, and Goswami [75] it very interesting. It talks of the monsoon variability as recurrent structures (although it never actually uses that name; they talk about quasiperiodic oscillations and "shades of active and break phases of the monsoon"). The first observational study I have found that approaches the oscillation in this manner.

They use Self Organizing Maps (SOM) to identify and classify different states of the intraseasonal variability. It seems to me that this might be a good way to sort out observations in a way that is closer to dynamical theories and to classify

recurrent structures (if one uses a more sophisticated technique). Maybe it is easier to find periodic orbits in climatic data sets in this way.

SOM is still not widely used in atmospheric science, much more emphasis is given to Empirical Orthogonal Functions. SOM seems to make more physical sense to me.